nature protocols

REVIEW ARTICLE

https://doi.org/10.1038/s41596-021-00551-z

Using single-vesicle technologies to unravel the heterogeneity of extracellular vesicles

Guillermo Bordanaba-Florit[1]✉, Félix Royo[1,2], Sergei G. Kruglik[3] and Juan M. Falcón-Pérez[1,2,4]✉

Extracellular vesicles (EVs) are heterogeneous lipid containers with a complex molecular cargo comprising several populations with unique roles in biological processes. These vesicles are closely associated with specific physiological features, which makes them invaluable in the detection and monitoring of various diseases. EVs play a key role in pathophysiological processes by actively triggering genetic or metabolic responses. However, the heterogeneity of their structure and composition hinders their application in medical diagnosis and therapies. This diversity makes it difficult to establish their exact physiological roles, and the functions and composition of different EV (sub)populations. Ensemble averaging approaches currently employed for EV characterization, such as western blotting or 'omics' technologies, tend to obscure rather than reveal these heterogeneities. Recent developments in single-vesicle analysis have made it possible to overcome these limitations and have facilitated the development of practical clinical applications. In this review, we discuss the benefits and challenges inherent to the current methods for the analysis of single vesicles and review the contribution of these approaches to the understanding of EV biology. We describe the contributions of these recent technological advances to the characterization and phenotyping of EVs, examination of the role of EVs in cell-to-cell communication pathways and the identification and validation of EVs as disease biomarkers. Finally, we discuss the potential of innovative single-vesicle imaging and analysis methodologies using microfluidic devices, which promise to deliver rapid and effective basic and practical applications for minimally invasive prognosis systems.

Since the description of 'minute bodies' found in a piece of cork by Robert Hooke in 1665[1], both our scientific knowledge and technical abilities have increased enormously. As techniques have become more accurate and intricate, so has our understanding of biological processes and structures. Technological advances in the field of imaging have resulted in the identification of cell structures, such as the mitochondria[2] and nuclei[3], and the discovery of different levels of cellular complexity. In 1967, Peter Wolf visualized 'platelet dust' in fresh platelet-free blood plasma using an electron microscope[4]; thus, a mammalian vesicle-like structure was described for the first time. Gradually, these vesicles were characterized in more detail. It has been established that they are released by all kinds of cells (prokaryotic and eukaryotic) into the extracellular milleu[5–8]. The process of vesicle secretion is conserved throughout evolution, suggesting that such vesicles are likely to have specific roles in cellular and organismal development and survival[9]. Indeed, later discoveries showed that secreted vesicles participate actively in many physiological processes in mammals, for example coagulation, inflammatory response, cell maturation, adaptive immune response, bone calcification and neural cell communication, among others[10,11]. In addition to their critical functions in normal physiology[12,13], secreted vesicles mediate in several pathological processes[14,15], such as the establishment of premetastatic niche during cancer progression[16,17].

Nowadays, these secreted vesicles are extensively reported and widely known as extracellular vesicles (EVs). EVs are heterogeneous, nano- to micrometer-sized, bilayer lipid containers secreted by most cell types. They are multipurpose carriers that can contain a wide variety of cargos such as lipids, proteins, metabolites, sugars, RNA (mRNA, miRNA, siRNA) and even DNA[10]. When they are taken up by recipient cells, they trigger intracellular signaling through EV surface molecules or by the release of cargo into cell compartments via endocytic pathways. These processes can further activate downstream genetic or metabolic pathways in the recipient cell[11,18]. In mammals, EVs have been found in body fluids such as plasma, urine, saliva, breast milk and seminal fluid, among others[10]. They are classified into three different categories according to their biogenesis mechanisms and biophysical properties:

- Exosomes: typically 30–150 nm in diameter, derived from intracellular endosomal compartments

[1]Exosomes Laboratory, Center for Cooperative Research in Biosciences (CIC bioGUNE), Basque Research and Technology Alliance (BRTA), Derio, Spain. [2]Centro de Investigación Biomédica en Red de Enfermedades Hepáticas y Digestivas (Ciberehd), Madrid, Spain. [3]Sorbonne Université, CNRS, Institut de Biologie Paris-Seine, Laboratoire Jean Perrin, Paris, France. [4]Ikerbasque, Basque Foundation for Science, Bilbao, Spain.
✉e-mail: gbordanaba@cicbiogune.es; jfalcon@cicbiogune.es

- Microvesicles: 100–1,000 nm in diameter, produced by outward budding and pinching-off the plasma membrane
- Apoptotic bodies: 50–5,000 nm in diameter, released as blebs by cells undergoing apoptosis[10,19]

In a systematic review of guidelines for this field, the International Society for Extracellular Vesicles (ISEV)[20] endorsed a categorization of EVs isolated using ultracentrifugation into large, medium and small EVs. However, it is important to note that ultracentrifugation precipitates not only vesicles but also lipoproteins, viruses, protein aggregates, ribonucleoprotein complexes and exomeres[21–23], which provides an additional layer or diversity but also a bias upon analysis of EV samples. Furthermore, there is evidence that exosomes, microvesicles and apoptotic bodies contain subpopulations with unique roles in biological processes[24,25]. These subpopulations are tightly integrated with a broad range of biological processes and exhibit a wide range of functionalities, which makes them an outstanding source of potential biomarkers for early diagnosis, drug delivery systems for therapeutics, or vaccine production systems[15,26–28].

During the last few decades, the interest in EVs and their applications has grown considerably. Many articles and reviews have focused on the functional role of EV heterogeneity. Their role in specific biological processes, such as cargo trafficking or regulation of signaling pathways, and their potential as biomarkers have also been examined[11,15,25,29,30]. Nonetheless, most of these studies examine the vesicles in bulk and use ensemble-averaging assays. Although such methods have been proven useful in specific cases, it is important to realize that the extensive heterogeneity of structure, composition and function of single vesicles is masked in such assays[24,29–31]. For example, the inability to detect the heterogeneity of molecular states of reaction pathways, individual proteins or nucleic acids may lead to a misinterpretation of ensemble measurements[32,33]. Recent developments in single-vesicle analysis (SVA) have opened new opportunities for the examination of heterogeneity within EV (sub)populations at the individual EV level and their characterization on the nanometer scale[9,29]. This new information is paramount for understanding the biological functions of EVs and for their potential clinical use.

Different EV populations and subpopulations can be isolated according to their physicochemical properties, yet the existing isolation technologies are intricate and still need to be further developed[24,29]. There are five main groups of techniques for sorting EV populations and subpopulations, based on ultracentrifugation, size, immunoaffinity capture, polymer precipitation and microfluidics[19]. Since each technique type sorts EVs using a different principle, each method can yield different EV subpopulations from the same sample[34,35]. Moreover, the highly concentrated EV preparations might contain contaminants, such as large protein aggregates and lipoproteins, left behind by some of the isolation techniques[36,37]. Interestingly, different approaches can also affect the physicochemical surface characteristics of EVs[38].

In consequence, some techniques tend to enrich or discriminate against specific EV populations. As sorting EVs into populations is usually based on physical properties only, we have to assume that such classification is largely arbitrary with respect to the composition or function of EVs. Vesicle isolation and enrichment techniques can help to yield more homogeneous EV subpopulations, albeit only for particular technique-specific parameters. In conclusion, although various isolation methods could help drive EV analysis toward a single-vesicle approach[9], many different compositions and functionalities are still expected to be found within such EV populations.

In this review, we describe the current methods used to study single-vesicles, and their contributions to the understanding of EV biology and biomarker discovery. Single-vesicle experiments can deliver direct information on the heterogeneous composition of EVs. They reveal multiple molecular states that govern EV functionality and transport and provide statistically valid information often lost in large ensemble experiments[19,29,39].

EV heterogeneity and biomarker discovery

There are many technological challenges to be met in the development of EV-based diagnostics. The relevant vesicles must be identified and isolated from complex biofluids, and a specific disease-related EV population or population mix has to be detected. Biomedical studies of EVs often focus on seeking suitable biomarkers for the diagnosis of various diseases[40,41]. For example, the functional role of EVs in various types of cancer has been extensively studied[14,16,17,27]. In this review, we concentrate on prostate cancer (PCa) diagnostics as an example application to which the SVA of EVs has made important contributions. According to the World Health Organization, PCa is among the most frequently diagnosed types of cancer, accounting for approximately a quarter of all cancer diagnoses in Europe[42], yet the lack of sensitive diagnostic tools and insufficient knowledge of the mechanisms of cancer emergence and progression are of major concern. PCa is a heterogeneous pathological state, both in the primary tumor in the prostate tissue and at the metastatic stage. It is unfortunately not advisable to examine PCa diversity relying solely on tissue biopsies, since these are highly invasive procedures and do not guarantee an effective and reliable diagnosis[43–46]. The serum prostate-specific antigen (PSA) test—still the cornerstone of PCa screening—is particularly questionable. Up to 40% of men undergo unnecessary biopsies as a result of poor specificity of the assay.

Remarkably, liquid biopsy has a potential for marker identification and provides better evidence of PCa diversity than the conventional solid tissue biopsy. In particular, prostate- and PCa-derived EVs and concomitant markers are highly abundant in urine, blood and ejaculate samples[47,48]. Hence, these body fluids could be used for detecting and measuring the progression of the disease. For example, the EVs released by PCa cells carry unique prostate-specific membrane proteins (e.g., TMPRSS2, STEAP2, PSMA, PPAP2A) that enable the detection of pathogenic prostate EVs and their capture for ex vivo characterization[49]. Although these data show that liquid biopsies may be highly informative and minimally invasive procedures, the methods for vesicle isolation, characterization and identification for disease diagnostics remain challenging. Up to date, there are no standardized

operating procedures for vesicle isolation and characterization for different types of samples and diseases, which complicates the employment of liquid biopsies as a clinical source for EV biomarkers.

SVA techniques for biological characterization of EVs

Most of the studies reviewed in this article examine the three problems that can be addressed by taking advantage of SVA techniques: (1) characterization of EV heterogeneity including subpopulations, surface (membrane protein and lipid) composition and vesicle content, (2) structural studies of EV membrane and soluble proteins and the assays to probe the metabolic activity of these proteins in a native-like environment and (3) characterization of the EV content and function depending on the cells of origin. The last task presents an interesting dichotomy: do the EVs reflect the properties of their cells of origin, or are they completely independent communication assets? On the one hand, it has been reported that EV surface and content depend on the parental cells[50–52]. On the other hand, some recent reports describe several EV subpopulations, with a range of different functionalities, originating from the same cell type[9,18,19,29,53,54]. Intriguingly, another recent article using SVA techniques demonstrates that the T2SS-like family of proteins is, in fact, responsible for selective cargo loading into EVs generated by the microorganism *Shewanella vesiculosa*[55].

Single-vesicle techniques

As increasing numbers of researchers have highlighted the importance of accurate EV (sub)population sorting and phenotyping, so far, more than 20 new single-vesicle techniques have been developed[9,19,29]. Many of these use microfluidic devices designed to integrate various technologies to improve EV sorting and detection. Moreover, several of these methods have been used for characterizing EVs at the single-vesicle level[56–67]. Some of these techniques can directly provide information on vesicle surface, content, size and shape, while others may require an upstream physicochemical characterization of the selected EV subpopulations to conduct surface profiling, monitor the expression of biomarkers and quantify them in body fluids. These technological advances should help to design new diagnostic devices for small sample sizes, using noninvasive or minimally invasive methods.

Twelve different methods are presented in Table 1 and discussed in detail in the following sections. Some of these methods utilize labeling techniques (such as fluorescence or nanoparticle coating) to visualize the EVs, and others work as label-free systems (Fig. 1). It is important to note that, in some cases, label-free approaches might hinder the detection of EVs because they often produce weak signals, which can be enhanced using a supporting labeling technique.

Label-free methodologies

Nanoparticle tracking analysis (NTA) is a technique based on the Brownian motion of microparticles in suspension, and it is used to determine the size distribution in particle populations[56,68]. In this approach, microparticles are detected by scattering the light of a laser beam, which is tracked and recorded at video frame rates. However, this approach has some disadvantages and limitations. For instance, the accurate assessment of particle size distribution requires specific track lengths, a steady temperature and a large number of replicates to provide robust results. Care should be taken when comparing different samples because variations in buffer viscosity and microparticle concentration introduce statistical errors. Moreover, the close proximity of two particles can result in overlap of the scattering signals. Accurate detection of particles with a diameter <60 nm is challenging, regardless of the NTA machine used[69]. Furthermore, vesicles cannot be discriminated from other particles, such as protein aggregates or virus particles. The vesicles can be probed specifically, and undesired particles excluded from the analysis only by employing fluorescent markers, yet only a fraction of EVs may carry known markers that can be used for labeling a specific subpopulation. General fluorescent labels (such as lipophilic carbocyanines DiO or DiI) can be used instead. However, it is important that any nonattached label be removed since this can mask the fluorescence signal emitted by labeled EVs[19].

Raman tweezers microspectroscopy (RTM), also known as laser tweezers Raman spectroscopy (LTRS), can be employed to examine the chemical content of EVs. This approach can be used to investigate both the surface and the internal volume of single EVs, revealing specific biomolecular signatures of proteins, lipids, nucleic acids and carotenoids as major contributors[57,60,61,70–77]. RTM is an inelastic scattering-based method. It employs a tightly focused laser beam for both optical trapping of single (or very few) vesicles in aqueous medium and excitation for subsequent Raman scattering, which provides a vibrational fingerprint from the trapped constituent biomolecules. The main inherent advantage of RTM lies in the signal linearity, which allows both qualitative and quantitative biochemical characterization of single EVs. This method is also label-free and provides data with high information content[57,71,74]. The main disadvantage is that the scattering efficiency is usually very low and thus provides a rather low level of informative Raman signal. As a result, an extended data collection time is required. Therefore, RTM, with a typical processing capacity of 0.2 particles per min, is not considered a high-throughput methodology[71]. RTM can, however, be used to obtain interesting, unique information not only for EVs[57,60,61,70–77] but also for many other bioparticles such as liposomes, lipid layers on synthetic nanoparticles and others[78–83].

Several methods have been developed to compensate for the low Raman signal strength in RTM. For example, the vesicle concentration can be increased by drop-coating deposition of the sample, followed by drying[84–88]. Unfortunately, this approach results in loss of information about individual EVs, as does any other analytical study of a bulk sample. Another strategy to increase the Raman signal is to use surface-enhanced Raman spectroscopy (SERS). In this method, EVs can be exposed to various signal-enhancing nanoparticles and/or substrates to obtain a strengthened biomolecular signal[62,89–95]. The main problem of label-free SERS is that the enhancement effect depends strongly on the distance between the biomolecule and the nanoparticle/substrate, and vanishes

Table 1 | Summary of main SVA techniques for individual EV characterization

Technique	Detection principle	Information obtained	Throughput	Time per analysis [a]	Sample preparation[b]	Is sample reusable?	Loading volume	Working concentration (mL^{-1})
High-resolution flow cytometry	Elastic light scattering; autofluorescence or fluorescence from external labels	Profiling[c] of EVs in a heterogeneous fluid mixture; functionalized fluorescent labels characterize specific populations	High	~1 min	Immunofluorescence or fluorescent conjugate staining protocol	No[d]	20–100 µL	10^7–10^{10}[e]
Nanoparticle tracking analysis	Imaging of Brownian motion pathways for EVs, using elastic light scattering or fluorescent labels	Particle concentration, size distribution	Moderate	~1 min	Dilution or concentration of Evs to the range optimal for the method	Yes	0.3–1.0 mL [f]	10^8–10^9
Raman tweezers microspectroscopy	Raman scattering from optically trapped single EVs	Biomolecular[g] composition of the surface and the interior of single EVs	Low	~1–5 min[h] per one[i] trapping event	Concentration of EVs to the range optimal for the method	Yes	~100 µL	10^7–10^{11} [j]
Surface-enhanced Raman spectroscopy (SERS)	Raman scattering enhanced by external active surface/coating	Partial [k] biomolecular[(g)] composition of the membrane of single EVs	Moderate	~1–10 s per one[(i)] EV	Fixation and coating protocol	No	50–100 µL	10^9–10^{11}
SERS with external labels	Enhanced Raman signal from SERS nanotags	Number of EVs with specific functionalized SERS nanotags attached	High	~10 s	Fixation and SERS-label staining	No	10–100 µL	10–10^7 [l]
Cryo-transmission electron microscopy (Cryo-TEM)	Transmission electron microscopy imaging	Morphological EV characterization[m]. Direct visualization of single EVs and examination of contaminants	Low	~1 h [(h)]	Vitrification of water in EVs dispersed on carbon grid, using fast-plunge freezing	No	2–10 µL	10^{10}–10^{12}
Atomic force microscopy (AFM)	Imaging (raster scanning) exploiting interaction force between the probing tip and immobilized EV	Precise [n] morphological, mechanical and biochemical [o] characterization of the EV surface	Low	~1 min per image[(i)]	Immobilization protocol.[p]	No	5–25 µL	Relative[q]

Table continued

Table 1 (continued)

Technique	Detection principle	Information obtained	Throughput	Time per analysis [a]	Sample preparation[b]	Is sample reusable?	Loading volume	Working concentration (mL^{-1})
Total internal reflection fluorescence microscopy (TIRF)	Imaging using fluorescence from external labels in an ultra-thin layer[r] of induced evanescent field[s]	Background fluorescence suppression; visualization of specific biomolecules[t] in vesicles of living cells; information on EV interaction and trafficking	Moderate	10–60 min	Fluorophore internalization protocol; calibration of the angle of incidence	Yes	10–200 µL	Relative[(q)]
Fluorescence resonance energy transfer (FRET)	Excitation energy transfer between donor and acceptor fluorophores via non-radiative resonance interaction; change[u] in fluorescence color	Structural information[v] derived from short-range[w] interactions in the donor–acceptor pair	Moderate	10–60 min	Fluorescence staining	Yes	10–200 µL	Relative[(q)]
Super-resolution microscopy	Fluorescence from external labels	Visualization of single vesicles in biological samples	Low	~1 s per image	Fluorescence staining; fixation protocol	No[x]	50–100 µL	Relative[(q)]
Droplet PCR	PCR amplification in partitions	Absolute quantification of specific targets in individual EVs or small *identical*[y] subpopulations	Moderate	~5 h per loading volume	EV droplet encapsulation protocol	No	20–150 µL	10^2–10^3
SP-IRIS	Enhanced scattering signal from particles bound to a substrate	Multiplexed phenotyping (surface biomarkers) and sizing of EVs populations in a single measurement	High	–	EV incubation on array	Yes	20 µL (microfluidics)	$<10^9$

[a]Time required for analysis once the sample and instrument are ready for the measurement. [b]Sample preparation protocol, for all techniques, contains the first obligatory step of EV purification and separation. [c]Obtaining size distribution, number of labeled particles, counting and sorting. [d]Attempts to sort the selected vesicles are under way and are likely to be successful in the future. [e]Dilution of the sample will be required to avoid swarm effect. [f]20 µL in microfluidics devices. [g]Distribution of proteins, lipids, nucleic acids, carotenoids and other biomolecules with pronounced, strong Raman bands. [h]Time for optimal working concentration. For particle concentration lower than optimal, the measurement time can increase considerably. [i]The total number of single EVs analyzed per sample depends on the task and measurement statistics and will be different for each particular experiment. [j]Concentration range is determined using the waiting time for the event of EV optical trapping. For larger/heavier EVs, lower concentrations are used: 10^7–10^9 mL^{-1} is suitable for large ~1 µm EVs, 10^8–10^{10} mL^{-1} is optimal for smaller exosomes, and up to 10^{11} mL^{-1} is required for the smallest (~50 nm) bioparticles. [k]Within the area of sufficient Raman-signal enhancement (depending on the geometry of interaction between EVs and the signal-enhancing surface/coating). [l]Exosome concentration logarithm is linear over the range of 40 particles/µL to 4×10^7 particles/µL plotted against Raman intensity[148]. [m]Polymorphism, membrane layers, internal-structure features, etc. [n]Lateral resolution 1–3 nm, axial resolution below 0.1 nm. [o]Using an immunofunctionalized probe tip. [p]On glass, mica or graphite (HOPG-type). [q]Working concentration spreads over a rather broad range and the optimal concentration strongly depends on EVs location in the microscope field. [r]Signal collection layer is usually less than ~100 nm thick, depending on the excitation wavelength and objective numerical aperture. [s]Evanescent field is created when the angle of incidence of excitation beam is larger than the angle of total reflection, so that the excitation beam does not penetrate into the sample. [t]miRNA, surface proteins. [u]Donor fluorescence disappears, acceptor fluorescence appears. [v]Assessment of conformational fluctuations, folding pathways, macromolecular interactions, kinetics of structural changes, etc. [w]When distance between donor and acceptor fluorophores becomes <8–10 nm. [x]Some SRM approaches damage the sample to such an extent that only one measurement is possible, and others permit several SRM-imaging analyses of a sample. [y]EV subpopulations with a specific surface protein in common.

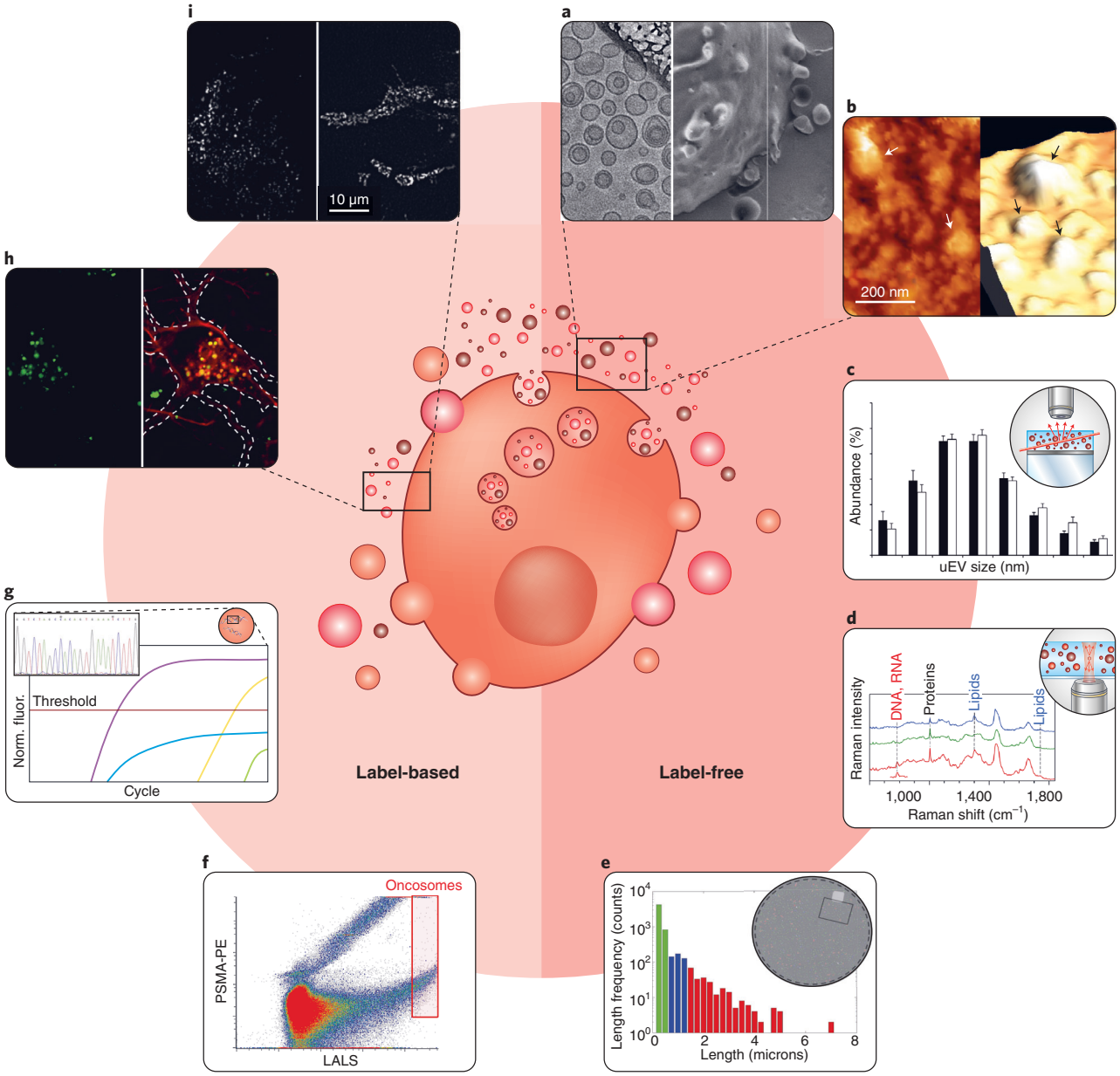

Fig. 1 | Schematic overview of the main SVA techniques discussed in this review. Data visualization and single-vesicle interpretation using each SVA methodology are depicted. In the center of the figure, a (tumorigenic) cell releasing EVs is shown. **a**–**i**, The techniques can be divided into two groups: label-free (**a**–**e**) and label-based (**f**–**i**) methodologies. The methods used here are cryo-electron microscopy[74,168] (**a**), AFM (**b**), NTA[9,172] (**c**), RTM[74] (**d**), SP-IRIS[111] (**e**), hrFC[223] (**f**), ddPCR[221] (**g**), SRM[130] (**h**) and fluorescence microscopy (**i**; TIRF image of synaptic vesicles is depicted)[253]. References show the source of the images. Panel **a** reprinted with permission from ref. [168]. Copyright 2017 Elsevier. Panel **d** reproduced from ref. [74]. Published by The Royal Society of Chemistry. Panels **c**–**i** reproduced with permission under Creative Commons Attribution 4.0 International License http://creativecommons.org/licenses/by/4.0/.

at distances longer than a few nanometers[89]. Therefore, this method is mainly suitable for characterization of biomolecules on the outer surface of EVs. In addition, Raman modes corresponding to molecular vibrations perpendicular to the SERS surface are preferably enhanced[89]. As a result, the overall SERS vibrational spectrum is usually somewhat distorted, lacks reproducibility and is often difficult to interpret.

In electron microscopy, a beam of electrons is emitted onto a sample in a vacuum environment. The wavelength of electrons is shorter than the visible light used in optical microscopy; thus, the method gives images of much higher resolution, typically below 1 nm[19]. Cryogenic transmission electron microscopy (cryo-TEM) is among the electron microscopy methods most commonly utilized for EV characterization. In contrast to the lengthy sample preparation needed for other TEM methods (usually taking hours), no heavy metals or fixatives are added, and no dehydration steps are required. This also limits sample damage and artifact effects, but yields lower-contrast images[96]. In cryo-TEM, the samples are prepared by rapid freezing, typically with liquid

ethane[57,97]. In this process, the water vitrifies, instead of forming ordered crystals, and the native structure of EVs is preserved[98]. The first exosome visualization was achieved using cryo-EM in 2008[99]. Since then, this technique has successfully revealed EV polymorphism by imaging the membrane bilayers, EV structures and internal features of individual EVs[57,63,96,100]. Even though cryo-TEM is an extremely useful technique for high-resolution visualization of EVs, this approach is relatively low-throughput. Cryo-TEM images typically only contain a few EVs (although the throughput could be enhanced by using automated search). In addition, cryo-TEM images provide only limited information regarding EV composition. To overcome this problem, nanoparticles functionalized with immunogold-labeled antibodies targeting markers of interest have recently been employed to characterize the biochemical composition of the EV surface[19,101].

Yet another type of microscopy method used for SVA is atomic force microscopy (AFM), which exploits the interaction between a probing tip and a sample surface. The deflection of the probing tip caused by interaction forces is detected and recorded using a laser and a sensor[102]. AFM allows an accurate morphological and mechanical characterization of EVs; its lateral resolution is 1–3 nm, and the vertical resolution <0.1 nm[102]. Typically, visualization of a few EVs using AFM is labor-intensive and time-consuming in comparison with other microscopy methods. However, a relatively high-throughput AFM-based method has been reported that measures the size and stiffness distribution of 100 vesicles within 1 h[65]. It is important to note that the tethering surface, to which the EV is bound, strongly affects the shape of the EVs. Therefore, the vesicles must be bound to a perfectly flat surface[103–105]. To characterize the biochemical properties of an EV surface, either the probing tip or the surface itself can be further (immuno)functionalized[106,107]. AFM can also be coupled with infrared spectroscopy (AFM-IR), allowing simultaneous measurements with a finer spatial resolution. AFM-IR has been extensively utilized in various applications; however, few papers report its implementation in the single-EV field[66,108]. We assume this is because the weak IR signal thwarts reliable characterization of individual vesicles.

Single-particle interferometric reflectance imaging sensor (SP-IRIS) is employed in assays based on interferometric imaging. It is used to detect individual enhanced scattering signals from the bound vesicle. The signals are produced by the interference between the scattered field from a vesicle and the reference field reflected off the layered substrate[109,110]. The method can detect several surface biomarkers and simultaneously measure the size of individual EVs. It can be used to accurately count and distinguish individual vesicles, with a low level of false positives and negatives[110]. However, as the lateral resolution of the microscope (~400 nm) could accommodate several small vesicles, some detected signals could be erroneously assigned and categorized as larger vesicles instead of several smaller vesicles. This could be an issue especially in highly concentrated sample preparations[111].

Label-based methodologies

Label-based methodologies are strongly dependent on the detection of a signal from a fluorescent protein, immuno- or lipophilic fluorophore or signal-enhancing nanoparticles. High-resolution flow cytometry (hrFC) is one of the first techniques extensively employed for individual EV analysis. hrFC can be used to quantify the size distribution and diversity of EV populations by detecting multiparametric scattered light and fluorescence emitted by the labeled vesicles. This fluorescence assay can be used to characterize the vesicle population by profiling the protein or nucleic acid content using antibody–fluorophore conjugates. However, any remaining free fluorescent dyes in the sample will cause high background fluorescence. This can be avoided by using density-based ultracentrifugation to purify labeled EVs, which leaves the nonreacted dye in the supernatant and sediments the vesicles into the pellet fraction[112,113]. Furthermore, multiple EVs (or particles) arriving simultaneously at the flow cytometer detector may be identified as single particles. This phenomenon is known as the swarm effect. The danger of such misidentification limits the concentration range within which the EVs (or particles) can be characterized effectively and makes it necessary to examine multiple diluted samples.

Fluorescence microscopy is an imaging technique particularly useful in localizing lipophilic fluorescent dyes or fluorescently labeled targets (either using fluorescent proteins or fluorescent dye-conjugated antibodies) in cells, tissues or EVs[9]. Another, rather elegant approach, now commonly used in the SVA field, is total internal reflection fluorescent (TIRF) microscopy. It can be used in an aqueous environment to image selectively the fluorescent molecules located near a highly refractive solid substance[114]. TIRF exploits the reflection of an excitation light beam at a high incident angle, typically between 60° and 80°, at which the beam of light is completely reflected by the glass–water interface. This reflection phenomenon generates a very thin electromagnetic field, called an evanescent wave, which is parallel to the substrate surface. This enables limited specimen illumination and thereby eliminates out-of-focus fluorescence and enhances the signal-to-noise ratio[115]. TIRF is predominantly used for studying intracellular single-vesicle processes such as endocytosis or exocytosis, cell–substrate contacts or internalization of plasma membrane receptors[114,115]. It can also directly localize fluorescently labeled molecules in EV preparations and allows tracking EVs in tissue preparations. However, the fluorophores can be excited only within a few hundred nanometers from the solid substrate, and the calibration of the incident angle can be difficult (depending on the setup)[114,115]. Moreover, the fluorophore instability and gradual photobleaching (although less pronounced than in other light microscopy techniques) during prolonged illumination might produce misleading results[9,116].

Fluorescence (or Förster) resonance energy transfer (FRET) is a phenomenon where the excitation energy from a fluorophore is transferred nonradiatively to another fluorophore. This happens via resonance energy transfer at distances <10 nm. FRET imaging offers unique opportunities for the assessment of kinetic and structural dynamics and studies of the interaction and fusion events between EVs and cells[117–119]. Notably, this imaging-based technique is capable of producing a considerable amount of single-particle and single-vesicle fluorescence data very fast[120–123]. However, fluorescent signal

fluctuations due to a low signal-to-noise ratio and poor photostability of certain dyes might lead to changes in the FRET signal that are unrelated to the biological processes. Like in other fluorescence-based techniques, the presence of multiple fluorophores within the observation volume may result in ensemble averaging of the population[119,124].

Super-resolution microscopy (SRM) is one of the most advanced applications of fluorescence imaging. It can be used to visualize biological features smaller than the optical diffraction limit and, therefore, below the conventional optical microscopy resolution limits (which are typically limited to ~250 nm axial and ~500 nm lateral resolution). This attribute provides an important advantage in imaging single EVs and permits investigation of their physiological functions[67,125–130]. Briefly, SRM techniques can be divided into two groups: (i) methods based on spatial patterning of the excitation light and (ii) methods based on single-molecule localization.

Excitation-patterning methods include structured illumination microscopy, in which the specimen is illuminated in a striped pattern[9,131] and stimulated emission depletion microscopy, which sharpens the excitation laser focus using a second laser that temporarily bleaches the fluorophores surrounding a small observation volume in the specimen[132,133].

Single-molecule localization methods detect fluorescence emitted from spatially isolated photo-switchable or blinking fluorophores to determine their position[133]. Photoactivation localization microscopy (PALM) relies on photoactivatable fluorescent recombinant proteins[134], whereas stochastic optical reconstruction microscopy (STORM) takes advantage of fluorophores that blink in a noncontrolled fashion. In both cases, only a small subset of fluorophores will be emitting simultaneously, allowing the precise localization of the fluorophores and reconstruction of the complete image at high spatial resolution[9]. Importantly, single-molecule localization approaches can be used in combination with TIRF, improving the signal-to-noise ratio and shortening imaging time[116]. Furthermore, all SRM techniques are based on the optics of classical diffraction-limited far-field light microscopes. This makes them compatible with existing sample preparation procedures, and also permits them access beyond the surface of a specimen. SRM techniques are also often minimally invasive[133,135]. It is important to note that most SRM approaches work only on fixed samples; thus, one should always be aware of potential artifacts introduced by the fixation method[9,136]. Another relevant aspect to consider is that, in general, the labeling of proteins using fluorescence markers or other tags might affect their localization, interaction partners and function[135]. In addition, although lipophilic or genetic labeling could allow visualization of single vesicles, lipid labeling in some cases might result in unspecific labeling or dye aggregates.

Digital droplet PCR (ddPCR) can be employed to distribute single EVs into individual droplets, which allows amplification and characterization of their genetic cargo[59,137,138]. Such cargo is usually RNA-based and mainly comprises miRNA, mRNA and noncoding RNA. In ddPCR, the EVs are tagged using anchoring molecules or antibodies and further distributed into microfluidic chambers according to their surface markers[59]. This methodology enables high-throughput quantitative analysis of EV content and can be used for the identification of biomarkers[139–142]. So far ddPCR use has been limited to validation purposes; however, it can be used as a screening technique (compromising its high-throughput capabilities)[19,143]. Interestingly, ddPCR has been already adopted for multiple mutation analysis to examine specific mutations in distinct populations of EVs. Next-generation sequencing could allow for parallel analysis of multiple mutations in many genes[144].

Finally, SERS nanotags functionalized with biorecognition molecules (such as target-specific antibodies) can be used to bind specifically to target EVs expressing the biomarker of interest. This approach is gradually becoming an important alternative to fluorescent molecular probes[94,145–149]. The major advantage of SERS labeling lies in the superior photochemical stability of Raman reporters compared with fluorescent labels, due to the vibrational nature of the generated signal. Moreover, several high-throughput Raman/SERS screening platforms for characterizing cells and EVs have been recently reported[70,150–153].

Recent advances in the EV field due to SVA

The recent breakthroughs in SVA techniques help to tackle the intrinsic limitations of ensemble EV measurements and analyses. In the following sections, we review the impact of SVA method development on recent advances and discoveries in the EV field (EV characterization, internalization, the role of EVs in cell-to-cell communication and biomarker discovery). In Table 2, we provide an overview of recent scientific articles describing the characterization of EVs, including studies of their heterogeneity and phenotyping of PCa-derived EVs. Current studies of EV internalization pathways and the role of EVs in cell-to-cell communication are summarized in Table 3. SVA techniques have been used in the successful identification and validation of a wide range of biomarkers for many different diseases. As an example, Table 4 lists recent discoveries in cancer research with a strong focus on PCa.

EV characterization

Several techniques mentioned in the previous section—NTA, cryo-TEM and flow cytometry—are established as customary characterization procedures for EV studies[141]. Notably, the results obtained employing these methodologies usually require validation using a complementary technique. This is because none of them is considered the gold standard procedure, and all of these approaches come with their own challenges and limitations[154]. For example, NTA is routinely utilized to obtain the size of EVs and quantify their abundance. However, since this technique is not vesicle-specific and can detect other particles, the reliability of the results must be cross-checked with other techniques. Therefore, EV studies that draw their conclusions solely from NTA are now uncommon, especially when compared with earlier EV characterization studies (from 2012 to 2015) when NTA was commonly utilized. Currently, NTA is often used as a supplementary characterization technique instead, as it requires minimal sample preparation to introduce fluorescent markers

Table 2 | Summary of EV characterization studies using SVA techniques

Technique	Main conclusion	Ref
AFM	The first time that plant exosomes have been visualized in their native state. They have been observed on the internal layers of the cell walls and their cargo assessed	156
	Matrix vesicles initiate changes during the mineralization of the extracellular matrix. In the course of this process, the matrix vesicles increase their size and crystallinity and change shape	157
AFM-IR	The first attempt to probe the differences between the molecular constituents (proteins, lipids and DNA) and structures of individual vesicles in two subtypes of placenta stem cells. In this work, protein aggregates have been successfully differentiated from vesicle structures	108
RTM	Vesicle shape and size depend on the lipid composition of the membrane. A decrease in cholesterol concentration increases the local membrane curvature and stretches the vesicle	82
Cancer research		
hrFC (immunofluorescence)	Microenvironment acidity of the prostate tumor increases the release of prostate-specific EVs	175
	EVs from PCa cells are very heterogeneous, but specific populations are not associated with different cancer stages. Mainly microvesicles and several exosome subpopulations are found, according to the surface signature	179
NTA	Increase in the number of released exosomes under acid pH (6.5), independent of tumor histotype	171
	Tumor cells release more EVs than do nontumorigenic cells (most likely due to the acidic environment in tumor cells)	174
Heterogeneity-related research		
NTA	Description of different EV populations in human glioblastoma cells	165
NTA (with fluorescence)	The first attempt to use this technique to determine the concentration and particle distribution in specific EV subpopulations, according to surface markers such as CD9, CD63, vimentin and LAMP-1	252
Electron microscopy (cryo-TEM)	Large diversity of exosome morphology revealed, regardless of the cell type and origin, suggesting that different exosome subpopulations from the same cell line perform different functions	96
	Visualization of a large spectrum of EVs from cerebrospinal fluid, including multilayer vesicles, single, double and double-membrane vesicles, and internal vesicular structures. These specific subpopulations are suggested to serve as potential biomarkers for Parkinson's disease	164
	Two different stimuli affecting EV release. Lipopolysaccharides and starvation conditions in human leukemia monocytic cell line (THP-1) affect the type of EVs shed and, probably, the shedding process	168
AFM	EVs isolated from different species are imaged. Using the tapping mode, the mechanical properties of EVs are assessed, concluding that the rat EVs are more fragile than the mouse vesicles	170
RTM	During cell growth and starvation-induced aggregation, *Dictyostelium discoideum* produces EVs that differ drastically in their biomolecular composition (nucleic acids, proteins, lipids, carotenoids)	57
	Detection of four EV populations with specific protein, phospholipid and cholesterol surface signatures. Their functionality determines their distribution; the populations are shared among several cell types	71
	In EV preparations from rat hepatocytes and human urine, single EVs from the same sample have different biochemical properties, well beyond the 'usual' variations for EVs from rat hepatocytes or human urine. A quantitative method developed to measure the concentration of nucleic acids in a single EV	74
	Combined morphochemical profiling of individual EVs is proposed based on Raman-enabled nanoparticle trapping analysis	75

for specific EV population studies. Likewise, labeling-based flow cytometry serves as a high-throughput sorting method for the characterization of certain EV features; however, it needs some technological improvements in separating unbound dye and dye aggregates from EVs to be utilized as a unique characterization approach[155]. Direct visualization of EVs using microscopy lets researchers assess the shape and size of vesicles in their native state[156] and in various biological processes[157], while other techniques, such as RTM, can be employed to examine further the morphology of bioparticles without direct visualization. For example, the effect of membrane lipid composition on the shape and size of giant unilamellar vesicles was first described using Raman tweezers, demonstrating that a decrease in cholesterol concentration increases the local membrane curvature and stretches the vesicle[82].

A large diversity in the morphology of exosomes has been reported for many types of cells[96]. For example, in the early 2010s, plasma EVs were comprehensively characterized and phenotyped using cryo-TEM in combination with gold nanoparticle-based immunolabeling[158]. This study found that

Table 3 | Mechanistic studies of vesicles using SVA techniques focusing on vesicle–cell communication, trafficking and vesicle fusion and endocytic pathways

Technique	Main conclusion	Ref
Vesicle–cell communication and trafficking research		
FRET microscopy	Tau protein misfolding and monomer aggregates spread in a prion-like manner causing neurodegenerative diseases such as Alzheimer's. Extracellular vesicles play a role in the transmission of pathological tau seeds	182
	The triad protein VOR is essential in the regulation of the endocytic nuclear transfer of EV-derived components. Targeting VOR might have therapeutic potential by inhibiting EV-mediated intracellular communication	185
Fluorescence microscopy (SRM)	In vivo visualization of EVs in the zebrafish embryo. Uptake of EVs by endothelial cells and blood patrolling macrophages is shown. The study demonstrates that tumor EVs activate macrophages and promote metastatic outgrowth	58
Electron microscopy (cryo-TEM)	Multiple virions and unique morphological components forming a mat-like structure are transported via infectious EVs of 100–1,000 nm in diameter. These infectious vesicles containing enterovirus material are secreted from host cells before lysis	184
ddPCR	EVs from osteotropic melanoma cells induce chemotaxis and cancer progression via upregulation of CXCR7 of nonosteotropic melanoma cells	186
Vesicle fusion and endocytic pathway research		
AFM	Description of mechanical properties of erythrocyte-derived EVs according to their protein–lipid ratio. While a high ratio is associated with soft vesicles, a low ratio corresponds to stiff EVs. These mechanical differences are linked to several vesiculation and budding mechanisms	187
Electron microscopy (cryo-TEM)	Visualization of the SNARE-mediated membrane fusion-by-hemifusion of small vesicles with cells shows fusion intermediates where lipid monolayers partially mix en route to complete bilayer merger	192
FRET microscopy	Description of the molecular mechanism of SNAREs during different membrane fusion stages, (docking, hemifusion and full fusion) by tracking the lipid-mixing process at the single-vesicle level	193
Fluorescence microscopy	The fusion pathways are heterogeneous, with an arrested hemifusion state predominating. The fusion of two lipid bilayers occurs spontaneously in a single step when they are brought into close proximity	191
Fluorescence microscopy (TIRF)	Heterogeneity of endocytic vesicle behaviors upon internalization. Prior to scission, vesicles remain proximal to the plasma membrane for variable periods. Clathrin uncoating is also variable	190
	Calcium activates synaptotagmin-1, resulting in SNARE-mediated fusion of synthetic vesicles used as an exocytic model for synaptic events. An optimal distance for the fusion is 5 nm	194
	Alterations in membrane cholesterol content shift hemifusion intermediates to full-fusion membrane and affect the stability of fusion pores. A large increase in cholesterol levels boosts individual SNARE-mediated fusion events	195
	Disassembly of the clathrin lattice surrounding coated vesicles is the obligatory last stage in their life cycle. The study visualizes the recruitment of auxilin and Hsc70, which is essential for this well-studied endocytic process	189
hrFC (fluorescent conjugates)	Characterization of microvesicles from red blood cells under stimulation and activation conditions. An increase in intracellular Ca^{2+} or protein kinase C levels leads to alterations in cell morphology and increased release of microvesicles	181
FRET microscopy	Free zinc concentration in insulin-storing vesicles is quantified using a novel FRET-based zinc sensor. The concentration of free zinc is important for insulin-storing vesicle maturity; hence, it alters insulin trafficking	180

platelet-free plasma samples contain a mixture of EVs with different morphologies, including spheres, cylinders and membrane fragments that are neither tubular nor spherical. Moreover, it has been shown that EVs come in a wide range of sizes[158]. Despite this morphological heterogeneity, only a minority of EVs in plasma expose phosphatidylserine on the surface. This is at odds with the classical theory of EV formation at the cell's plasma membrane, in which the loss of phospholipid asymmetry and exposure of phosphatidylserine precedes membrane blebbing and shedding[159–163]. The authors have suggested that some EV (sub)populations ought to be generated and regulated via different pathways[158]. Likewise, Emelyanov et al. have described a large spectrum of EV morphologies and (sub)populations after isolating EVs from cerebrospinal fluid and visualizing them using cryo-TEM[164]. They have reported several different morphologies, including multilayered, single- and double-membrane vesicles, as well as internal vesicular structures. Interestingly, a subpopulation

Table 4 | Summary of recent EV biomarker-related discoveries achieved using SVA techniques, focused on cancer diagnostic biomarkers

Technique	Main conclusion	Ref
Flow cytometry (immunofluorescence)	Detection of CD147 as EV biomarker for CRC diagnosis	208
	Detection of GPC1 as EV biomarker for pancreatic cancer diagnosis. Cancer-cell EVs contain oncogenic KrasG12D	222
	Measures circulating PMP levels in plasma. This PCa 'liquid biopsy' can identify patients with Gleason score $\geq$ 8, irrespective of their PSA	223
Fluorescence microscopy (TIRF)	Employs a fluorescent assay to detect exosome miRNA-21 (miR-21-EX) as a cancer-screening assay. miR-21-EX can be used to distinguish between cancer patients, tumor progression stages and treatment responses	211
Raman (dry EVs)	The surface protein signature shifts from alpha-helix-rich proteins to beta-sheet-rich proteins in PCa-specific blood EVs	84
RTM	Chemical signatures from Raman spectra can be used to differentiate between EV populations derived from healthy and PCa cells. A trained convolutional neural network can identify the cellular origin of EVs	73,77
RTM	Raman analysis coupled with Rayleigh scattering distribution is used to detect specific lipid and protein signatures of tumor-derived EVs	76
Label-free SERS	Report of real-time and label-free diagnosis of lung cancer by detecting 11 cancer-specific SERS signals (proteins and lipids) that distinguish EV populations from healthy and lung cancer cells with high sensitivity	92
ddPCR	Detection and quantification of mutant and wild-type IDH1 RNA transcripts in EVs from cerebrospinal fluid of patients with glioma tumors	140
	Identifies somatic BRAF and KRAS mutations in plasma-derived EVs from CRC patients. Probes a wide range of cancer cells and the derived EV populations	221
	Identifies KLK3 and AR-V7 (androgen receptor variant) as biomarkers for castration-resistant PCa (which progresses even under steroid deprivation therapy)	216
	Extracellular vesicle-transported HULC promotes cell invasion and migration. This encapsulated HULC is identified as a biomarker for human pancreatic ductal adenocarcinoma	142

of these EVs plays a key role in Parkinson's disease progression[164]. Another study, using NTA-based technology, has identified several EV populations released by human glioblastoma cells[165]. Moreover, fluorescence-based NTA approaches are being used to examine the concentration and particle distribution of specific EV subpopulations[166,167].

The relative chemical abundance of major biomolecules comprising EVs, namely proteins, lipids, nucleic acids and carotenoids, can be obtained from the vibrational fingerprints acquired using RTM. Tatischeff et al. have shown that *Dictyostelium discoideum* in two different physiological states (i.e., cell growth and starvation-induced aggregation) produce EVs with drastically different biomolecular compositions[57]. In another study, Smith et al. have categorized four EV populations according to specific protein, phospholipid and cholesterol vibrational signatures, which are shared among several cell types from different species[71]. The authors have found that human lung carcinoma A549, human hepatocarcinoma Huh-7 and mouse embryonic fibroblast 3T3 cells have similar EV populations. In contrast, Kruglik et al. have reported direct Raman evidence of pronounced biomolecular heterogeneity of single EVs in the same sample (using rat hepatocytes and human urine)[74]. In their study, the heterogeneity was determined by quantitative measurements of nucleic acid concentration within single EVs, based on the intensity of the pyrimidine ring stretching band[74].

Further heterogeneity studies performed with cryo-TEM and AFM have described the physical characteristics of EVs. One cryo-TEM analysis has reported that the shedding process and, hence, the type of EV released is strongly affected by external stimuli, such as lipopolysaccharides or starvation conditions, in a human leukemia cell line[168]. By using the tapping mode in AFM, biomechanical properties such as elasticity, stiffness and deformability of single EVs can be assessed[169]. It has been reported that rat hepatocyte-derived EVs are more fragile and easily warped than liver-progenitor mouse EVs[170]. Another study performed using AFM-IR has allowed, for the first time, probing of molecular constituents and structures of individual vesicles[108]. In this study, the researchers were able to differentiate between the molecular compositions of EVs derived from two subtypes of placenta stem cells. Moreover, their approach has allowed discrimination between protein aggregates and EVs. The examination of DNA, lipids and proteins using AFM-IR, in just a few vesicles, has remarkable potential in early disease diagnosis[108].

SVAs have been extensively utilized in cancer research, for example, to characterize the EVs in PCa. NTA-based research has established that cancer cells produce larger amounts of EVs than do nontumorigenic cells[47,171,172] and that low extracellular pH increases the release of EVs from cancer cells[173,174]. Interestingly, NTA studies also support the idea

that tumorigenic cells upregulate EV production owing to the acidification of the immediate microenvironment[175–178]. Logozzi et al. have employed a combination of hrFC and immunofluorescence to discover that acidic microenvironment of prostate tumors induces the release of PCa-specific EVs[175]. These EVs are very heterogeneous, and several populations can be identified, according to their surface composition. However, it is important to note that this heterogeneity is not related directly to different cancer stages[179].

In summary, the highlighted reports of single-EV characterization demonstrate that EV morphology and composition are largely independent of cell origin and that certain EV (sub) populations are involved in various diseases. These discoveries indicate that morphologically different EV populations may be distributed according to their specific function and biogenesis pathway, rather than the cell type of their origin.

EV trafficking and signaling mechanisms

SVA approaches have advanced EV research by tracking particular molecules and examining the changes in cells under different conditions. Early in 2020, FRET studies in T cells showed that the concentration of free zinc in cells is a major regulator of the maturation process in insulin-storing vesicles[180]. SVA has also contributed to discoveries reporting an increase in intracellular Ca^{2+} and/or protein C under certain stimulating and activating conditions in red blood cells. These conditions alter cell morphology and cause an increase in the release of microvesicles[181]. Table 3 summarizes more examples of recent advances in research in (a) vesicle–cell communication and trafficking and (b) vesicle fusion and endocytic pathways.

EVs serve as information carriers for cell pathways and may trigger some diseases due to this activity. Neurodegenerative diseases such as Alzheimer's are caused by the misfolding and aggregation of tau protein. Polanco et al. have described a prion-like spread of tau protein seeds brought about by EVs, employing cryo-TEM[182] and SRM (PALM and STORM)[130]. The contribution of EVs to trans-synaptic tau transmission has been confirmed using cryo-TEM in another study[183]. This single-vesicle methodology has also been utilized recently to study the near-native 3D architecture of EVs secreted after infection with poliovirus. Cryo-TEM tomography has generated images of virions and viral structures contained in EVs before cell lysis[184]. Moreover, FRET microscopy has been used to track the triad protein VOR (paramount for the transfer of EV-derived components to the nucleus)[185]. This type of research has therapeutic potential for diminishing the progression of neurodegenerative diseases (in the case of the VOR complex, by inhibiting EV-mediated intercellular communication).

Cancer mechanisms have also been analyzed using single-molecule techniques. Mannavola et al. performed a ddPCR experiment using osteotropic melanoma cells and observed that EVs could induce the upregulation of genes such as CXCR7[186]. Thus, EVs may act as chemotaxis agents and, hence, participate in the progression of cancer; however, additional research in this field is still required to achieve better understanding of how EVs contribute to cancer[186].

Vesicle budding and shedding and the mechanical properties of the vesicles are poorly understood. Remarkably, a recent comparative review suggests that biomechanical analysis of single EVs provides key insights into their biological structure, biomarker functions and potential therapeutic functions[169]. Sorkin et al. used AFM to study these properties in erythrocyte and EV membranes under different conditions[187]. They established that stiffness is inversely proportional to the protein–lipid ratio and linked it to several different budding mechanisms[187]. On the one hand, budding of protein-rich soft vesicles is possibly driven by protein aggregation, and on the other, budding of stiff vesicles with low membrane-protein content is likely to be driven by cytoskeleton-induced buckling[187]. A further investigation comparing EVs originating from healthy erythrocytes and from those with hereditary spherocytosis has supported these observations. It also uncovered mechanical and vesiculation differences between these two EV populations with potential use as diagnostic parameters[188].

Vesicle endocytic pathways have been investigated primarily using microscopy-based techniques. One major EV endocytosis pathway is mediated by the formation of clathrin-coated vesicles (Fig. 2b). In this process, intracellular clathrin interacts with the membrane, producing a membrane invagination that will form an endosome through which the EVs can be internalized. The disassembly of the clathrin lattice surrounding coated endosomes is a mandatory last step in their life cycle. The recruitment of auxilin and Hsc70 (fluorescently labeled) was directly visualized using an inverted fluorescence microscope equipped with TIRF hardware and described as essential for clathrin-based internalization events[189]. The clathrin-driven uncoating is a variable process in which the endocytosing clathrin-coated vesicles remain proximal to the membrane for different periods prior to the scission of plasma membrane. The dynamics of clathrin-mediated endocytosis were assayed using fluorescently tagged proteins and TIRF microscopy[190].

Fusion states, dynamics and mechanisms of vesicle internalization during single-vesicle fusion events have been directly examined using cryo-TEM, FRET and TIRF microscopy. Characteristics and kinetics of individual fusion events can be quantified for the lipids or DNA–lipid complexes involved in the process. Different fusion pathways exist: vesicles and cell membrane merge via a direct fusion of membranes (Fig. 2a) or using protein-mediated mechanisms (Fig. 2c). These mechanisms are involved in both endocytosis and exocytosis events. Examining individual giant unilamellar vesicles by fluorescence microscopy, it has been shown that, during a direct fusion event, the hemifusion state predominates, and the fusion of two bilipid layers occurs in a single step when they are sufficiently close[191].

During the last decade, the fusion mechanism based upon SNARE-mediated internalization pathways (Fig. 2c) has been investigated employing SVA. At the molecular level, SNARE proteins mediate vesicle fusion with the target membrane and with membrane-bound compartments. Recently, Mattie et al. visualized SNARE single-fusion events using cryo-TEM[192]. The sequence of fusion intermediates from lipid monolayers to a

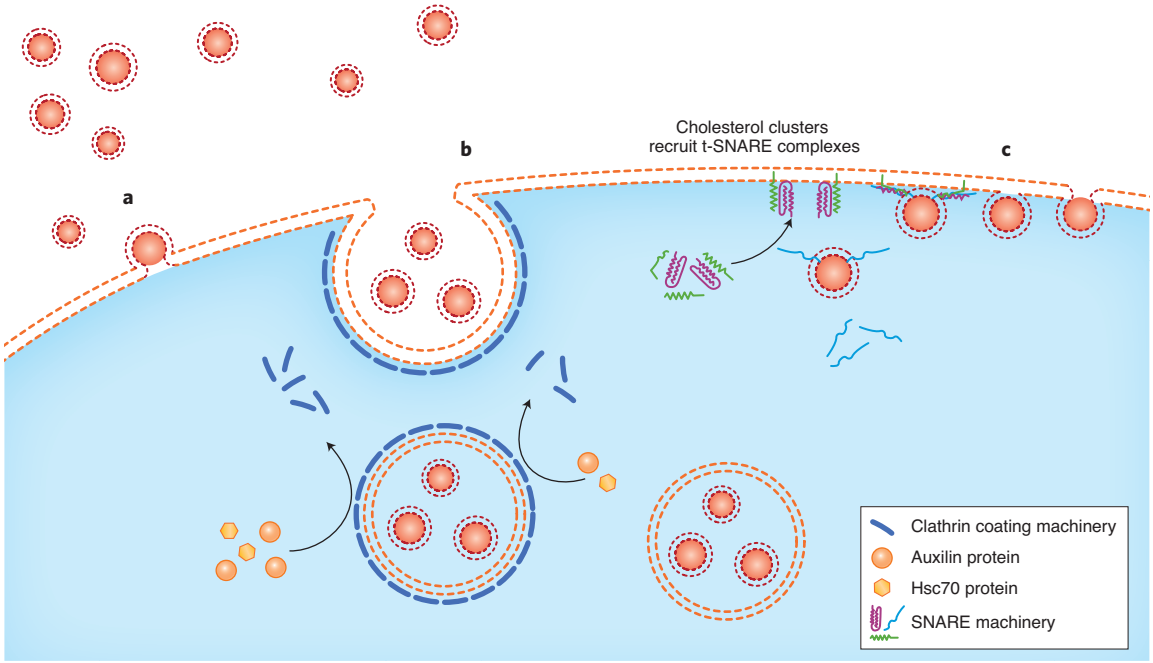

Fig. 2 | Schematic representation of endocytic and fusion pathways recently investigated using SVA techniques. A lipid bilayer from a recipient cell is shown in dotted orange, and EV lipid bilayer in dotted red; the intracellular content is shaded in blue, and vesicle content in red. **a**, direct fusion of EVs with the plasma membrane[191]. **b**, Clathrin-based internalization[189,190]. TIRF microscopy allows the examination of the clathrin uncoating process. **c**, SNARE-mediated membrane fusion[192]. FRET microscopy facilitates the analysis of the three main stages of endocytic and fusion pathways: docking, hemifusion and full fusion. Membrane composition enhances this fusion pathway through t-SNARE-machinery recruitment and enrichment[195].

complete bilayer merge has been reported in homotypic vacuoles[192]. Hu et al. correlated the membrane fusion stages with a molecular mechanism using reconstituted vesicles[193]. At a single-vesicle level, they traced the lipid-mixing process using FRET microscopy and correlated it with the docking, hemifusion and full-fusion stages[193]. They also report that an optimal distance for a SNARE-mediated fusion is 5 nm. Interestingly, some regulators of fusion pathways were identified in related studies. Calcium acts as an activator of synaptotagmin-1, leading to the fusion of synaptic vesicles with the presynaptic membrane[194]. Stratton et al. identified cholesterol as an important regulator of fusion dynamics, shifting the process from hemifusion intermediates toward full-fusion membranes[195]. Large amounts of cholesterol precluster t-SNAREs, which serve as functional docking and fusion platforms. These clusters substantially affect the stability of pores by increasing the fraction of fully open pores and accelerating fusion events. Consequently, high cholesterol content triggers fast and individual SNARE-mediated fusion events[195].

During the last decade, multimodal imaging platforms have been tested in vitro in a number of different cellular models of disease[196–198]. These platforms have considerable potential to be used in vivo, for instance, in mice[199–202]. However, these systems usually fail to perform single-EV tracking and have been successful only in ex vivo cultures[196]. Nevertheless, there is an animal model worth mentioning owing to its physiological characteristics and transparency. Zebrafish embryo has emerged recently as a prospective model for tracking EVs and assessing their dissemination and uptake in vivo[203,204]. In 2019, Hyenne et al. reported an approach for tracking individual circulating tumor EVs in the zebrafish embryo[58] using confocal microscopy and a combination of chemical and genetically encoded probes to image EVs in vivo. The authors described, for the first time, the hemodynamic behavior of tumor EVs and their intravascular arrest. The study shows that the endothelial cells and blood macrophages rapidly take up circulating tumor EVs. These EVs activate blood patrolling macrophages and promote metastatic outgrowth[58]. A back-to-back study performed by Verweij et al. combined the genetic labeling (using a CD63-pHluorin exosomal reporter) of specific tissues with electron microscopy to track endogenous EVs in blood and further unravel their mechanisms of biogenesis, biodistribution and target cells throughout the zebrafish embryo[203]. Intriguingly, Sung et al. recently reported a CD63-pHluorin-mScarlett fusion protein that can be used to image several stages of the exosome lifecycle in vitro[205]. This reporter likely can be used to visualize exosomes in vivo and is a prospective tool for underFstanding the physiological roles of exosomes.

EV biomarkers

SVA techniques hold the capacity to discover new, specific and effective biomarkers in EVs that have been missed by ensemble methods and can be used in disease diagnostics. While the resolution and sensitivity of SVA techniques still needs improving, they provide an accurate characterization of EV subpopulations and assessment of biomarkers. Extensive research has been carried out seeking the biological biomarkers for several diseases such as PCa[47,151,172], fibromyalgia[206],

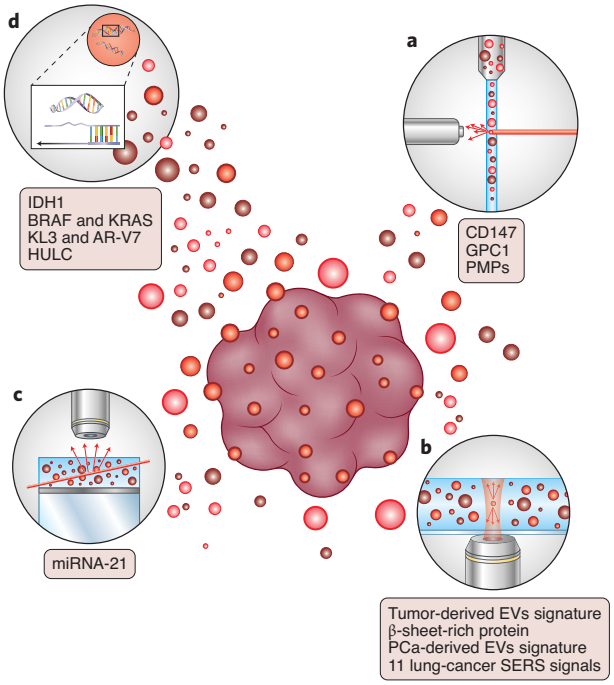

Fig. 3 | Schematic overview of reviewed biomarkers discovered using SVA techniques. a–d, The methods shown here are hrFC[208,222,223] (**a**), RTM[61,73,77,84,92] (**b**), TIRF[207] (**c**) and ddPCR (**d**) [140,142,216,221]. More information for specific biomarkers discovered using each method can be found in Table 4.

endometrial cancer[207], colorectal cancer (CRC)[208,209] and liver-associated diseases[210], among others. Figure 3 summarizes recent advances in cancer research at the single-vesicle level. Currently, fluorescent assays, which are often used in cancer screening[211], can detect miRNAs and correlate their presence with individual EVs and EV populations. Exosome-localized miRNA-21 might be used to differentiate between cancer patients and assess tumor progression and response to treatment[211]. Moreover, a specific lipid–protein signature may identify tumor-derived EVs as Raman spectra within the range of 2,800–3,100 cm^{-1} appear to be a distinguishing feature of genuine cancer EVs.[76]. These findings open the way for early cancer detection. Nevertheless, the biomarkers discussed here are either generic (cannot discriminate between different cancers) or come from 2D cancer model research and might not adequately diagnose clinical cancers.

The development of next-generation sequencing SVA methods has optimized the identification of cancer biomarkers. Specifically, targeted sequencing using cancer gene panels has allowed the study of EV-derived and circulating free DNA[144], resulting in the discovery of genetic biomarkers for several diseases. For instance, nine miRNAs have been profiled in serum EVs. Using these profiles, chronic hepatitis C patients can be distinguished from healthy individuals with accuracy >95%[212]. Diagnostic opportunities presented by EV-specific genetic biomarkers have been widely reviewed[213–216]. It has been shown that cancer-derived EVs rewire and modify the premetastatic microenvironment, supporting tumor growth and metastasis during cancer progression[14,17,18,139]. This research describes a set of potential marker targets to be used as early diagnosis of PCa. The promotion and proliferation of PCa triggered by EVs produced as a result of DIAPH3 loss or growth factor stimulation have also been reported[139]. Other studies have shown that miRNA quantification in tissues can identify PCa by detecting the expression of RNU24[217] or miR-130b[218].

Recently, several studies have reported specific and sensitive biomarkers for cancer detection[92,140,142,219–222]. ddPCR has detected and quantified the IDH1 transcript in cerebrospinal fluid-derived EVs of patients with glioma tumors in the brain[140]. In lung cancer, 11 cancer-specific SERS signals have been obtained, allowing differentiation between EV populations derived from healthy and lung cancer cells with high sensitivity[92]. Additionally, the CD147 protein found in EVs has been identified as a biomarker for CRC diagnosis[208]. Further studies have identified BRAF and KRAS somatic mutations in plasma-derived EV populations from CRC patients[221]. Intriguingly, Melo et al. have described an explicit biomarker, glypican 1 (GPC1), found in EV populations from pancreatic cells containing different KRAS oncogenic isomers[222]. Hence, GPC1-EV identification could facilitate early pancreatic cancer diagnosis[222]. In 2020, the EV-transported HULC lncRNA (long noncoding RNA highly upregulated in liver cancer) was suggested as a chemotaxis agent for cell invasion and migration. This encapsulated HULC is a potential biomarker for human pancreatic adenocarcinoma diagnosis[142].

The recent advances in cancer biomarker research are a proof-of-concept for noninvasive diagnostic tools based on EV fingerprinting in combination with multivariate statistical analysis[62]. The investigations in the field of noninvasive diagnostics for PCa have been stimulated by the discovery of intrinsic biomarkers detected in urinary-derived EVs. As a result of SVA research, several biomarkers have been associated with different stages of PCa. Biggs et al. have measured the levels of circulating prostate microparticles (PMPs) in plasma from PCa patients[223] and used these microparticles in a liquid biopsy platform to identify and characterize patients. This study found that subjects with an advanced and aggressive tumor (in Gleason scale, scoring 8 or higher) can be identified independently of their PSA value[223]. The lipid and surface protein signatures of prostate-derived EVs have been described using Raman and RTM[60,73,77,84]. Several characteristics have been highlighted indicating potential PCa biomarkers. For example, a shift in the structure of surface proteins from alpha-helix-rich in prostate EVs to beta-sheet-rich proteins in PCa-specific EVs (isolated from blood samples) has been observed[84]. Moreover, Otto et al. have detected chemical signatures in Raman and Rayleigh scattering data[73] that efficiently differentiate between the EV populations from normal prostate and PCa cells[61,76]. The authors have trained a convolutional neural network to predict precisely the cellular origin of EVs for an automated diagnosis of PCa[77]. In another study, using various SVA techniques such as nanoscale flow cytometry and ddPCR, Joncas et al. have explored castration-resistant PCa[216], identifying KLK3 and the androgen receptor variant 7 (AR-V7) as specific biomarkers for this type of cancer[216].

Future outlook

Individually analyzed EVs provide excellent prospects for future basic and practical research with a view to halt disease progression and control cell-to-cell communication processes. To exploit the full potential of SVA techniques, biological validation and reproducibility must meet the demands of clinical applications. Each technique has its specific advantages and disadvantages, and the exact choice of the method of analysis depends on the research question, the nature of the samples and EV characteristics. These techniques still need to improve their quantitative detection power, lower their cost and increase the reliability, resolution and throughput. In addition to technologies already in use for SVA detection, we highlight several promising approaches that have yet to prove their potential in SVA.

Conventional methodologies have the potential to be applied in SVA, and flow cytometry is a good example. Its implementation using innovative approaches can provide new features and capabilities, as shown by vesicle impact electrochemical cytometry (VIEC). This electrochemistry-based flow cytometry technique uses single ruptured vesicles whose content is detected and quantified based on Faraday's law exploiting the produced oxidation current[224,225]. Extensive studies of the regulation of neurotransmitter trafficking by Ewing and colleagues, focusing on catecholamine exocytosis [226–234], have demonstrated the prospective application of this approach in the EV field, highlighting electrochemical flow cytometry as a prospective asset in studies of EV functions and biology in the near future. The VIEC-based experiments have examined neurotransmitter content at a single-vesicle level in a pheochromocytoma cell line. Several studies have established that the neurotransmitter catecholamine is only partially released from the vesicles during an exocytosis event[229]. Moreover, catecholamine concentration is a key factor in regulating vesicle size since vesicular transmitter content is relatively constant and independent of vesicle size[230]. Nonetheless, many different agents may regulate exocytosis events. Using VIEC, the group later verified that the zinc and cisplatin content serve as major regulators in these processes[231,232].

Video microscopy is another common technique that is potentially useful in EV analysis. In 2010, Zupanc et al. developed an efficient algorithm to transform video sequences into quantitative data[233]. Their work was a crucial step toward the creation of automated computer analysis and led to the development of another, more popular, methodology, NTA. In 2008, the then-emerging fluorescent ratiometric image analysis (FRIA) method was used to determine the postendocytic fate and transport kinetics of internalized cargo[234]. FRIA presented a breakthrough in this field at the time, and its application led to colocalization of EV cargo with organelle markers. However, the technique has not been very successful in further EV research, possibly owing to the emergence of other microscopy approaches such as TIRF or SRM that enable the study of EV internalization and fate with a better resolution in fluorescence images and a more straightforward analysis.

The last decade has seen the development of several techniques with primary applications in analytical fields other than EV analysis. However, some—most notably radiofrequency analysis and SP-IRIS—are applicable to single-vesicle research and could play an important role in scanning and evaluation of specific EV populations or characterizing several EV parameters in a single experiment.

Radiofrequency analysis, also known as electrically controlled tuneable broadband interferometric dielectric spectroscopy, has only been presented in several conference papers[235–238] after its first publication. In this method, specific sensors are used to perform a highly sensitive and tuneable broadband radiofrequency analysis. One study applying this method to EVs showed that the highly concentrated radiofrequency fields stimulate strong interactions between vesicles, which can be detected and quantified[239]. Specifically, the authors could detect and scan a type of EV, giant unilamellar vesicles, at multiple frequency points and determine their molecular composition. In 2017, Wu et al. reported a separation method based on acoustofluidics and created a platform employing the so-called acoustic trapping or tweezers phenomenon[240]. This technique isolates EVs from whole blood in a label-free and contact-free manner[240]. An acoustic wave falls upon a vesicle, and its scattering acts as a driving force to retain the EVs. A year later, Ku et al. demonstrated isolation and enrichment of EVs using a similar acoustic trap technology[241]. In follow-up research, the method was used to isolate RNA and sequence miRNAs from EVs. Since then, an acoustic-based microfluidic platform has been released, coupling EV trapping technology with next-generation sequencing techniques. Together, these platforms form a robust and automated strategy for biomarker discovery in small sample volumes[242].

SP-IRIS has so far found limited use in EV research, but has the potential to fill a unique experimental niche. SP-IRIS can characterize the size and phenotype (surface biomarkers) of EVs with no need to correlate two separate measurements[64,110]. This feature provides SP-IRIS with a high throughput and substantially reduces the amount of false negatives and positives compared with techniques that assess two characteristics in individual measurements. Due to the lateral resolution of microscopy (340–435 nm), highly concentrated samples cause signal overlap and a subsequent shift in the apparent vesicle size. Strikingly, despite the microscope resolution drawback, individual *Flaviviridae* particles of ~40 nm have been identified and characterized using SP-IRIS[111]. Besides the examples presented in Table 5, there is a commercialized platform for EV phenotyping developed by Nanoview Biosciences using SP-IRIS, highlighting its potential application in characterizing limited input EV samples. Several papers have proposed other highly promising automated on-chip platforms using SP-IRIS for EV characterization[64,111,243–245]. These platforms have been combined with immunoblotting to sort and characterize EV populations from a sample and can detect size and phenotype at a single-particle level, visualizing and quantifying either viruses or single EVs, or both, in an uncharacterized sample.

One of the greatest advantages of such microfluidic platforms is that they need only very small sample volume (~20 μL) for an effective analysis[244,246]. Other techniques different from SP-IRIS have been implemented in such devices to characterize EVs from EV-regulated diseases and examine their future use as diagnostic tools. EVs derived from

Table 5 | Summary of on-chip platforms utilized to characterize EVs and to detect specific biomarkers using SVA techniques

On-chip technique	Objective	Description	Ref
Dark-field microscopy and immunoelectrophoresis	Surface protein/marker profiling of EV populations	On-chip immunoelectrophoresis device that separates EV populations according to the zeta potential of their surfaces (due to overexpression of certain markers) and quantifies the populations. This is a promising approach for minimally invasive diagnosis of cancer	245
SP-IRIS and immunoplotting	Sizing and phenotyping at single exosome level	Multiplexed phenotyping and digital counting of various populations of individual exosomes (<50 nm) captured on a microarray-based solid phase chip	64
SP-IRIS and immunoplotting	Visualizing and quantifying virus particles with a single label-free imaging technique	A silicon chip with virus-specific antibodies on printed spots can visualize and identify intact Ebola viruses and Ebola virus-like particles without labeling. The device also performs an automated quantitative analysis of the captured viruses	243
SP-IRIS and immunoplotting	Sizing, phenotyping and quantifying EVs and virus populations	Multiplexed detection technology based on protein immobilization on a sensor chip. DNA-directed immobilized antibodies are used to design protein microarrays to capture EVs or viruses. Several types of analytes in a small volume can be simultaneously characterized using SP-IRIS	244
Nanoflow cytometry and fluorescence microscopy	Automated lab-on-a-chip quantitative analytical tool for SVA	A nanofluidic device that can visualize and characterize individual vesicles by quantifying vesicle content and fluorescence signals from sample volumes of 20 μL. This nanofluidic-based methodology can be used for characterization of small vesicles and their interacting molecules without ensemble averaging	246
Atomic force microscopy (AFM) and nanopatterned tethering	Morphological and deformability characterization of single EVs from different cell lines	A nanoarray chip allows tethering of individual EVs from two cell lines (Sk-Br-3 and HEK293), employing a silane-coupling agent as a linker between PEG-lipid molecules and silicon surface. These tethered EVs are further characterized using AFM	248
Raman/SERS screening	Identification and quantification of EV surface biomarkers in cancer	A microfluidic device performs a rapid (8 min) and ultrasensitive identification, comparable to ELISA, of specific biomarkers in several samples at the same time. Protein biomarkers for prostate (PSA), colorectal (CEA), and hepatocellular prostate (AFP) cancers are detected	151
Raman imaging, SEM, AFM combined with immunoplotting	Size distribution, shape and chemical fingerprint characterization of tumor-derived EVs	Multimodal analysis platform that captures specifically tumor-derived EVs on an antibody-functionalized stainless-steel chip. A lipid–protein fingerprint is obtained using Raman imaging, and the particle distribution and surface density are measured employing SEM and AFM. The correlation between SEM and Raman discriminates tumor derived EVs from contaminants. This device is tested using PCa cell lines	70,152
Multicolor fluorescence digital PCR	Highly sensitive detection (compared with qPCR) of cancer-specific gene expression	The miDER chip multiplex assay is an innovative digital PCR method capable of detecting and quantifying extremely low quantities of EV-related RNA. It can measure expression levels of two lung cancer-related genes (SLC9A3-AS1 and PCAT6) in peripheral blood samples, with a limit of detection of 10 copies per μL	250
SP-IRIS and atomic force microscopy (AFM) with immunoplotting	Investigates whether plasma- or activated platelet-EVs trigger NETs	Plasma transfusion can cause TRALI mediated by NETs. NanoBioAnalytical platform based on EV immunocapture biochip can detect EVs with a diameter in the 25–1,000 nm range (mainly ≤100 nm). The study shows that EVs from both plasma and activated platelets trigger NET formation	247
Antibody barcodes (immuno-sandwich ELISA)	Quantification and phenotyping of EV secretion	Microchip platform for multiplexed profiling of single-cell EV secretion, using antibody barcodes. This technology addresses the heterogeneity of EVs of the same origin. For example, the study shows that protein and EV secretion is performed mostly by certain cell subgroups	249

transfusion-related acute lung injury (TRALI) have been investigated using SP-IRIS coupled with AFM mechanics. Obeid et al. used this approach to determine that certain types of EVs trigger neutrophil extracellular traps (NETs) and that these NETs are likely to mediate in TRALI[247].

Fluorescence microscopy coupled with on-chip nanoflow cytometry enables automated quantitative SVA of body fluid samples[246]. According to Yokota et al., the morphology and deformability of EVs from different cell lines can be investigated using nanopatterned tethering of EVs in combination

with AFM[248]. A multiplexed profiling antibody-based barcoding method enables sorting and further quantification of EV populations[249]. Notably, promising minimally invasive approaches for cancer detection and analysis have also been developed. For example, a multicolor fluorescence digital PCR platform has been designed to detect the expression of cancer-specific genes with high sensitivity[250]. This platform detects miRNA, lncRNA or any other genetic biomarkers of cancer. Furthermore, several devices for PCa detection have been described. For instance, EV populations from PCa can be separated according to the zeta potential of the surface and examined using dark-field microscopy[251]. Due to the over-expression of certain markers, different numbers of antibodies are bound to the EV surfaces, modifying their surface potential. This implies that EVs are differentially separated according to this potential. The biochemical composition of each EV is profiled and quantified; hence, subpopulations can be described. Moreover, two RTM approaches that can effectively identify and quantify EVs and their surface biomarkers in several cancers have been reported[151,152]. Beekman et al. have presented a multimodal analysis platform combining Raman imaging, scanning electron microscopy, AFM and immunoblotting as the ultimate PCa diagnosis platform capable of measuring size distribution, shapes and chemical fingerprints of tumor-derived EVs[152].

The remarkable advances in single-vesicle imaging and analysis brought about by employing microfluidic devices promise to deliver rapid and effective practical applications. Moreover, such analytical systems need only very small, microliter-scale sample volumes. These innovative technologies and affiliated research pave the way toward unraveling the biological significance of EVs and using minimally invasive systems to diagnose diseases for which EVs serve as prognostic biomarkers.

Concluding remarks

EVs are key drivers of cell-to-cell communication. Understanding their biochemistry and physiological roles is paramount for unraveling biological processes such as disease progression, physiological responses or environmental regulation. EVs are also remarkably heterogeneous, which often complicates their accurate analysis by bulk and ensemble studies that often misrepresent their functionalities. Indeed, EVs comprise several populations that further branch into subpopulations according to their morphology or phenotype. These (sub)populations could have specific functions, or several (sub)populations might perform the same task as an amalgam. It is now becoming clear that not only the phenotype of an EV community but also its relative representation among the rest of the (sub)populations might be of importance. Studies using SVA methodologies represent the most encouraging attempts toward highlighting and pinpointing specific EV phenotypes within a biological system. While SVA methods are well suited for the high-resolution phenotypical characterization of EVs that is necessary for biomarker discovery, they might not be appropriate for carrying out further functional studies. So far, these methods have only been successful in identifying the uptake and fusion pathways, but future advances in system models or single-vesicle technology may encourage their wider use. Ultimately, single-vesicle techniques will provide the foundation for describing an entirely new cell-to-cell communication paradigm built upon an EV-based network.

References

1. Hooke, R. *Micrographia: or Some Physiological Descriptions of Minute Bodies Made by Magnifying Glasses. With Observations and Inquiries Thereupon* (1665).
2. Die Altmann, R. *Elementarorganismen und ihre Beziehungen zu den Zellen* (von Veit, 1890).
3. van Leeuwenhoek, A. *Opera Omnia, seu Arcana Naturae ope exactissimorum Microscopiorum detecta, experimentis variis comprobata, Epistolis ad varios illustres viros.*
4. Wolf, P. The nature and significance of platelet products in human plasma. *Br. J. Haematol.* **13**, 269–288 (1967).
5. Herr, D. R. et al. Ultrastructural characteristics of DHA-induced pyroptosis. *Neuromolecular Med.* https://doi.org/10.1007/s12017-019-08586-y (2020).
6. Patras, L. & Banciu, M. Intercellular crosstalk via extracellular vesicles in tumor milieu as emerging therapies for cancer progression. *Curr. Pharm. Des.* **25**, 1980–2006 (2019).
7. Andaloussi, S. E. L., Mäger, I., Breakefield, X. O. & Wood, M. J. A. Extracellular vesicles: biology and emerging therapeutic opportunities. *Nat. Rev. Drug Discov.* **12**, 347–357 (2013).
8. Buzas, E. I., György, B., Nagy, G., Falus, A. & Gay, S. Emerging role of extracellular vesicles in inflammatory diseases. *Nat. Rev. Rheumatol.* **10**, 356–364 (2014).
9. Panagopoulou, M. S., Wark, A. W., Birch, D. J. S. & Gregory, C. D. Phenotypic analysis of extracellular vesicles: a review on the applications of fluorescence. *J. Extracell. Vesicles* **9**, 1710020 (2020).
10. Yáñez-Mó, M. et al. Biological properties of extracellular vesicles and their physiological functions. *J. Extracell. Vesicles* **4**, 27066 (2015).
11. Van Niel, G., D'Angelo, G. & Raposo, G. Shedding light on the cell biology of extracellular vesicles. *Nat. Rev. Mol. Cell Biol.* **19**, 213–228 (2018).
12. Nieuwland, R. & Sturk, A. Why do cells release vesicles? *Thromb. Res.* **125**, S49–S51 (2010).
13. Valadi, H. et al. Exosome-mediated transfer of mRNAs and microRNAs is a novel mechanism of genetic exchange between cells. *Nat. Cell Biol.* **9**, 654–659 (2007).
14. Anderson, H. C., Mulhall, D. & Garimella, R. Role of extracellular membrane vesicles in the pathogenesis of various diseases, including cancer, renal diseases, atherosclerosis, and arthritis. *Lab. Investig.* **90**, 1549–1557 (2010).
15. Wiklander, O. P. B., Brennan, M., Lötvall, J., Breakefield, X. O. & Andaloussi, S. E. L. Advances in therapeutic applications of extracellular vesicles. *Sci. Transl. Med.* **11**, 1–16 (2019).
16. An, T. et al. Exosomes serve as tumour markers for personalized diagnostics owing to their important role in cancer metastasis. *J. Extracell. Vesicles* **4**, 27522 (2015).
17. Becker, A. et al. Extracellular vesicles in cancer: cell-to-cell mediators of metastasis. *Cancer Cell* **30**, 836–848 (2016).
18. Zhao, H. et al. Tumor microenvironment derived exosomes pleiotropically modulate cancer cell metabolism. *eLife* **5**, e10250 (2016).
19. Chiang, C. Y. & Chen, C. Toward characterizing extracellular vesicles at a single-particle level. *J. Biomed. Sci.* **26**, 9 (2019).
20. Théry, C. et al. Minimal information for studies of extracellular vesicles 2018 (MISEV2018): a position statement of the International Society for Extracellular Vesicles and update of the MISEV2014 guidelines. *J. Extracell. Vesicles* **7**, 1535750 (2018).

21. Zhang, H. et al. Identification of distinct nanoparticles and subsets of extracellular vesicles by asymmetric-flow field-flow fractionation. *Nat. Cell Biol.* **20**, 332–343 (2018).
22. Mathieu, M., Martin-Jaular, L., Lavieu, G. & Théry, C. Specificities of secretion and uptake of exosomes and other extracellular vesicles for cell-to-cell communication. *Nat. Cell Biol.* **21**, 9–17 (2019).
23. Tai, Y. L., Chen, K. C., Hsieh, J. T. & Shen, T. L. Exosomes in cancer development and clinical applications. *Cancer Sci.* **109**, 2364–2374 (2018).
24. Willms, E., Cabañas, C., Mäger, I., Wood, M. J. A. & Vader, P. Extracellular vesicle heterogeneity: subpopulations, isolation techniques, and diverse functions in cancer progression. *Front. Immunol.* **9**, 738 (2018).
25. Kalluri, R. & LeBleu, V. S. The biology, function, and biomedical applications of exosomes. *Science* **367**, eaau6977 (2020).
26. Van Der Pol, E. et al. Optical and non-optical methods for detection and characterization of microparticles and exosomes. *J. Thromb. Haemost.* **8**, 2596–2607 (2010).
27. Soung, Y. H., Ford, S., Zhang, V. & Chung, J. Exosomes in cancer diagnostics. *Cancers (Basel)* **9**, 8 (2017).
28. Puente-Massaguer, E., Lecina, M. & Gòdia, F. Application of advanced quantification techniques in nanoparticle-based vaccine development with the Sf9 cell baculovirus expression system. *Vaccine* **38**, 1849–1859 (2020).
29. Pick, H., Alves, A. C. & Vogel, H. Single-vesicle assays using liposomes and cell-derived vesicles: from modeling complex membrane processes to synthetic biology and biomedical applications. *Chem. Rev.* **118**, 8598–8654 (2018).
30. Tkach, M., Kowal, J. & Théry, C. Why the need and how to approach the functional diversity of extracellular vesicles. *Philos. Trans. R. Soc. B Biol. Sci.* **373**, 20160479 (2018).
31. Goñi, F. M. The basic structure and dynamics of cell membranes: an update of the Singer-Nicolson model. *Biochim. Biophys. Acta* **1838**, 1467–1476 (2014).
32. Bhatia, V. K. et al. Amphipathic motifs in BAR domains are essential for membrane curvature sensing. *EMBO J.* **28**, 3303–3314 (2009).
33. Mathiasen, S. et al. Nanoscale high-content analysis using compositional heterogeneities of single proteoliposomes. *Nat. Methods* **11**, 931–934 (2015).
34. Brett, S. I. et al. Immunoaffinity based methods are superior to kits for purification of prostate derived extracellular vesicles from plasma samples. *Prostate* **77**, 1335–1343 (2017).
35. Royo, F. et al. Different EV enrichment methods suitable for clinical settings yield different subpopulations of urinary extracellular vesicles from human samples. *J. Extracell. Vesicles* **5**, 29497 (2016).
36. Ramirez, M. I. et al. Technical challenges of working with extracellular vesicles. *Nanoscale* **10**, 881–906 (2018).
37. Sódar, B. W. et al. Low-density lipoprotein mimics blood plasma-derived exosomes and microvesicles during isolation and detection. *Sci. Rep.* **6**, 24316 (2016).
38. Woo, J. R., Sharma, S. & Gimzewski, J. The role of isolation methods on a nanoscale surface structure and its effect on the size of exosomes. *J. Circ. Biomark.* **5**, 11 (2016).
39. Takahashi, K., Yan, I. K., Kim, C., Kim, J. & Patel, T. Analysis of extracellular RNA by digital PCR. *Front. Oncol.* **4**, 129 (2014).
40. Liu, Y. & Lu, Q. Extracellular vesicle microRNAs: biomarker discovery in various diseases based on RT-qPCR. *Biomark. Med.* **9**, 791–805 (2015).
41. Giannopoulou, L., Zavridou, M., Kasimir-Bauer, S. & Lianidou, E. S. Liquid biopsy in ovarian cancer: the potential of circulating miRNAs and exosomes. *Transl. Res.* **205**, 77–91 (2019).
42. Crocetti, E. *Epidemiology of prostate cancer in Europe*. Centre for Parliamentary Studies https://ec.europa.eu/jrc/en/publication/epidemiology-prostate-cancer-europe (2015).
43. Torrano, V. et al. Vesicle-MaNiA: extracellular vesicles in liquid biopsy and cancer. *Curr. Opin. Pharmacol.* **29**, 47–53 (2016).
44. Heidenreich, A. et al. EAU guidelines on prostate cancer. Part 1: screening, diagnosis, and local treatment with curative intent—update 2013. *Eur. Urol.* **65**, 124–137 (2014).
45. Humphrey, P. A. Diagnosis of adenocarcinoma in prostate needle biopsy tissue. *J. Clin. Pathol.* **60**, 35–42 (2007).
46. Shariat, S. F. & Roehrborn, C. G. Using biopsy to detect prostate cancer. *Rev. Urol.* **10**, 262–280 (2008).
47. Clos-Garcia, M. et al. Metabolic alterations in urine extracellular vesicles are associated to prostate cancer pathogenesis and progression. *J. Extracell. Vesicles* **7**, 1470442 (2018).
48. Höög, J. L. & Lötvall, J. Diversity of extracellular vesicles in human ejaculates revealed by cryo-electron microscopy. *J. Extracell. Vesicles* **4**, 28680 (2015).
49. Duijvesz, D. et al. Immuno-based detection of extracellular vesicles in urine as diagnostic marker for prostate cancer. *Int. J. Cancer* **137**, 2869–2878 (2015).
50. Raposo, G. & Stoorvogel, W. Extracellular vesicles: exosomes, microvesicles, and friends. *J. Cell Biol.* **200**, 373–383 (2013).
51. Raposo, G. & Stahl, P. D. Extracellular vesicles: a new communication paradigm? *Nat. Rev. Mol. Cell Biol.* **20**, 509–510 (2019).
52. Théry, C., Clayton, A., Amigorena, S. & Raposo, G. Isolation and characterization of exosomes from cell culture supernatants. in *Current Protocols in Cell Biology* https://doi.org/10.1002/0471143030.cb0322s30 (2006).
53. Giulietti, M. et al. Exploring small extracellular vesicles for precision medicine in prostate cancer. *Front. Oncol.* **8**, 221 (2018).
54. Russell, A. E. et al. Biological membranes in EV biogenesis, stability, uptake, and cargo transfer: an ISEV position paper arising from the ISEV membranes and EVs workshop. *J. Extracell. Vesicles* **8**, 1684862 (2019).
55. Chen, C. et al. Isolation of a novel bacterial strain capable of producing abundant extracellular membrane vesicles carrying a single major cargo protein and analysis of its transport mechanism. *Front. Microbiol.* **10**, 3001 (2020).
56. Szatanek, R. et al. The methods of choice for extracellular vesicles (EVs) characterization. *Int. J. Mol. Sci.* **18**, 1153 (2017).
57. Tatischeff, I., Larquet, E., Falcon-Perez, J. M., Turpin, P.-Y. & Kruglik, S. G. Fast characterisation of cell-derived extracellular vesicles by nanoparticles tracking analysis, cryo-electron microscopy, and raman tweezers microspectroscopy. *J. Extracell. Vesicles* **1**, 19179 (2012).
58. Hyenne, V. et al. Studying the fate of tumor extracellular vesicles at high spatiotemporal resolution using the zebrafish embryo. *Dev. Cell* **48**, 554–572.e7 (2019).
59. Tian, Q. et al. Nanoparticle counting by microscopic digital detection: selective quantitative analysis of exosomes via surface-anchored nucleic acid amplification. *Anal. Chem.* **90**, 6556–6562 (2018).
60. Carney, R. P. et al. Multispectral optical tweezers for biochemical fingerprinting of CD9-positive exosome subpopulations. *Anal. Chem.* **89**, 5357–5363 (2017).
61. Enciso-Martinez, A. et al. Synchronized Rayleigh and Raman scattering for the characterization of single optically trapped extracellular vesicles. *Nanomedicine* **24**, 102109 (2020).
62. Stremersch, S. et al. Identification of individual exosome-like vesicles by surface enhanced raman spectroscopy. *Small* **12**, 3292–3301 (2016).
63. Yuana, Y. et al. Cryo-electron microscopy of extracellular vesicles in fresh plasma. *J. Extracell. Vesicles* **2**, 21494 (2013).
64. Daaboul, G. G. et al. Digital detection of exosomes by interferometric imaging. *Sci. Rep.* **6**, 37246 (2016).
65. Ridolfi, A. et al. AFM-based high-throughput nanomechanical screening of single extracellular vesicles. *Anal. Chem.* **92**, 10274–10282 (2020).

66. Kim, S. Y., Khanal, D., Kalionis, B. & Chrzanowski, W. High-fidelity probing of the structure and heterogeneity of extracellular vesicles by resonance-enhanced atomic force microscopy infrared spectroscopy. *Nat. Protoc.* **14**, 576–593 (2019).
67. Zong, S. et al. Single molecule localization imaging of exosomes using blinking silicon quantum dots. *Nanotechnology* **29**, 065705 (2017).
68. Filipe, V., Hawe, A. & Jiskoot, W. Critical evaluation of nanoparticle tracking analysis (NTA) by NanoSight for the measurement of nanoparticles and protein aggregates. *Pharm. Res.* **27**, 796–810 (2010).
69. Bachurski, D. et al. Extracellular vesicle measurements with nanoparticle tracking analysis—an accuracy and repeatability comparison between NanoSight NS300 and ZetaView. *J. Extracell. Vesicles* **8**, 1596016 (2019).
70. Rikkert, L. G. et al. Cancer-ID: toward identification of cancer by tumor-derived extracellular vesicles in blood. *Front. Oncol.* **10**, 608 (2020).
71. Smith, Z. J. et al. Single exosome study reveals subpopulations distributed among cell lines with variability related to membrane content. *J. Extracell. Vesicles* **4**, 28533 (2015).
72. Carney, R. P. et al. Targeting tumor-associated exosomes with integrin-binding peptides. advanced biosystems. *Physiol. Behav.* **1**, 1600038 (2017).
73. Lee, W. et al. Label-free prostate cancer detection by characterization of extracellular vesicles using Raman spectroscopy. *Anal. Chem.* **90**, 11290–11296 (2018).
74. Kruglik, S. G. et al. Raman tweezers microspectroscopy of circa 100 nm extracellular vesicles. *Nanoscale* **11**, 1661–1679 (2019).
75. Dai, Y. et al. Combined morpho-chemical profiling of individual extracellular vesicles and functional nanoparticles without labels. *Anal. Chem.* **92**, 5585–5594 (2020).
76. Enciso-Martinez, A. et al. Label-free identification and chemical characterisation of single extracellular vesicles and lipoproteins by synchronous Rayleigh and Raman scattering. *J. Extracell. Vesicles* **9**, 1730134 (2020).
77. Lee, W., Lenferink, A. T. M., Otto, C. & Offerhaus, H. L. Classifying Raman spectra of extracellular vesicles based on convolutional neural networks for prostate cancer detection. *J. Raman Spectrosc.* **51**, 293–300 (2020).
78. Bryce, D. A., Kitt, J. P. & Harris, J. M. Confocal-Raman microscopy characterization of supported phospholipid bilayers deposited on the interior surfaces of chromatographic silica. *J. Am. Chem. Soc.* **140**, 4071–4078 (2018).
79. Kitt, J. P., Bryce, D. A., Minteer, S. D. & Harris, J. M. Confocal Raman microscopy for in situ measurement of phospholipid-water partitioning into model phospholipid bilayers within individual chromatographic particles. *Anal. Chem.* **90**, 7048–7055 (2018).
80. Penders, J. et al. Single particle automated Raman trapping analysis. *Nat. Commun.* **9**, 4256 (2018).
81. Bour, A. et al. Lipid unsaturation properties govern the sensitivity of membranes to photoinduced oxidative stress. *Biophys. J.* **116**, 910–920 (2019).
82. Collard, L., Sinjab, F. & Notingher, I. Raman spectroscopy study of curvature-mediated lipid packing and sorting in single lipid vesicles. *Biophys. J.* **117**, 1589–1598 (2019).
83. Bryce, D. A., Kitt, J. P., Myres, G. J. & Harris, J. M. Confocal Raman microscopy investigation of phospholipid monolayers deposited on nitrile-modified surfaces in porous silica particles. *Langmuir* **36**, 4071–4079 (2020).
84. Krafft, C. et al. A specific spectral signature of serum and plasma-derived extracellular vesicles for cancer screening. *Nanomed. Nanotechnol., Biol. Med.* **13**, 835–841 (2017).
85. Gualerzi, A. et al. Raman spectroscopy uncovers biochemical tissue-related features of extracellular vesicles from mesenchymal stromal cells. *Sci. Rep.* **7**, 9820 (2017).
86. Gualerzi, A. et al. Raman spectroscopy as a quick tool to assess purity of extracellular vesicle preparations and predict their functionality. *J. Extracell. Vesicles* **8**, 1568780 (2019).
87. Zhang, H., Silva, A. C., Zhang, W., Rutigliano, H. & Zhou, A. Raman spectroscopy characterization extracellular vesicles from bovine placenta and peripheral blood mononuclear cells. *PLoS ONE* **15**, e0235214 (2020).
88. Morasso, C. F. et al. Raman spectroscopy reveals biochemical differences in plasma derived extracellular vesicles from sporadic amyotrophic lateral sclerosis patients. *Nanomedicine* **29**, 102249 (2020).
89. Cialla, D., Pollok, S., Steinbrücker, C., Weber, K. & Popp, J. SERS-based detection of biomolecules. *Nanophotonics* **3**, 383–411 (2014).
90. Lee, C. et al. 3D plasmonic nanobowl platform for the study of exosomes in solution. *Nanoscale* **7**, 9290–9297 (2015).
91. Fazio, B. et al. SERS detection of biomolecules at physiological pH via aggregation of gold nanorods mediated by optical forces and plasmonic heating. *Sci. Rep.* **6**, 26952 (2016).
92. Park, J. et al. Exosome classification by pattern analysis of surface-enhanced Raman spectroscopy data for lung cancer diagnosis. *Anal. Chem.* **89**, 6695–6701 (2017).
93. Rojalin, T., Phong, B., Koster, H. & Carney, R. P. Nanoplasmonic approaches for sensitive detection and molecular characterization of extracellular vesicles. *Front. Chem.* **7**, 729 (2019).
94. Wang, J., Koo, K. M., Wang, Y. & Trau, M. Engineering state-of-the-art plasmonic nanomaterials for SERS-based clinical liquid biopsy applications. *Adv. Sci.* **6**, 1900730 (2019).
95. Pramanik, A. et al. Mixed-dimensional heterostructure material-based SERS for trace level identification of breast cancer-derived exosomes. *ACS Omega* **3**, 16602–16611 (2020).
96. Zabeo, D. et al. Exosomes purified from a single cell type have diverse morphology. *J. Extracell. Vesicles* **6**, 1329476 (2017).
97. Orlov, I. et al. The integrative role of cryo electron microscopy in molecular and cellular structural biology. *Biol. Cell* **109**, 81–93 (2017).
98. Dubochet, J. et al. Cryo-electron microscopy of vitrified specimens. *Q. Rev. Biophys.* **21**, 129–228 (1988).
99. Conde-Vancells, J. et al. Characterization and comprehensive proteome profiling of exosomes secreted by hepatocytes. *J. Proteome Res.* **7**, 5157–5166 (2008).
100. Zonneveld, M. I. et al. Recovery of extracellular vesicles from human breast milk is influenced by sample collection and vesicle isolation procedures. *J. Extracell. Vesicles* https://doi.org/10.3402/jev.v3.24215 (2014).
101. Cizmar, P. & Yuana, Y. Detection and characterization of extracellular vesicles by transmission and cryo-transmission electron microscopy. in *Extracellular Vesicles: Methods and Protocols* (eds. Kuo, W. P. & Shidong, J.) 221–232 (Springer, 2017).
102. Binnig, G., Quate, F. & Gerber, C. Atomic force microscope. *Phys. Rev. Lett.* **56**, 930–933 (1986).
103. Sharma, S. et al. Structural-mechanical characterization of nanoparticle exosomes in human saliva, using correlative AFM, FESEM, and force spectroscopy. *ACS Nano* **4**, 1921–1926 (2010).
104. Parisse, P. et al. Atomic force microscopy analysis of extracellular vesicles. *Eur. Biophys. J.* **46**, 813–820 (2017).
105. Creasey, R. et al. Atomic force microscopy-based antibody recognition imaging of proteins in the pathological deposits in pseudoexfoliation syndrome. *Ultramicroscopy* **111**, 1055–1061 (2011).
106. Sebaihi, N., De Boeck, B., Yuana, Y., Nieuwland, R. & Pétry, J. Dimensional characterization of extracellular vesicles using atomic force microscopy. *Meas. Sci. Technol.* **28**, 034006 (2017).
107. Skliar, M. & Chernyshev, V. S. Imaging of extracellular vesicles by atomic force microscopy. *J. Vis. Exp.* https://doi.org/10.3791/59254 (2019).

108. Kim, S. Y., Khanal, D., Tharkar, P., Kalionis, B. & Chrzanowski, W. None of us is the same as all of us: Resolving the heterogeneity of extracellular vesicles using single-vesicle, nanoscale characterization with resonance enhanced atomic force microscope infrared spectroscopy (AFM-IR). *Nanoscale Horiz.* **3**, 430–438 (2018).
109. Avci, O., Ünlü, N. L., Özkumur, A. Y. & Ünlü, M. S. Interferometric reflectance imaging sensor (IRIS)—a platform technology for multiplexed diagnostics and digital detection. *Sensors* **15**, 17649–17665 (2015).
110. Trueb, J. T., Avci, O., Sevenler, D., Connor, J. H. & Ünlü, M. S. Robust visualization and discrimination of nanoparticles by interferometric imaging. *IEEE J. Sel. Top. Quantum Electron.* https://ieeexplore.ieee.org/document/7782781 (2017).
111. Daaboul, G. G. et al. Enhanced light microscopy visualization of virus particles from Zika virus to filamentous ebolaviruses. *PLoS ONE* **12**, e0179728 (2017).
112. van der Vlist, E. J., Nolte-'t Hoen, E. N. M., Stoorvogel, W., Arkesteijn, G. J. A. & Wauben, M. H. M. Fluorescent labeling of nano-sized vesicles released by cells and subsequent quantitative and qualitative analysis by high-resolution flow cytometry. *Nat. Protoc.* **7**, 1311–1326 (2012).
113. Gomes, J. et al. Analytical considerations in nanoscale flow cytometry of extracellular vesicles to achieve data linearity. *Thromb. Haemost.* **118**, 1612–1624 (2018).
114. Fish, K. N. Total internal reflection fluorescence (TIRF) microscopy. *Curr. Protoc. Cytom.* https://doi.org/10.1002/0471142956.cy1218s50 (2009).
115. Kudalkar, E. M., Davis, T. N. & Asbury, C. L. Single-molecule total internal reflection fluorescence microscopy. *Cold Spring Harb. Protoc.* **2016**, pdb.top077800 (2016).
116. Axelrod, D. Chapter 7: total internal reflection fluorescence microscopy. *Methods Cell Biol.* **89**, 169–221 (2008).
117. Ha, T. Single-molecule fluorescence resonance energy transfer. *Methods* **25**, 78–86 (2001).
118. Arluison, V. & Wien, F. *RNA Spectroscopy: Methods and Protocols* (Springer, 2020).
119. Cerdán, L. et al. FRET-assisted laser emission in colloidal suspensions of dye-doped latex nanoparticles. *Nat. Photonics* **6**, 621–626 (2012).
120. Rectenwald, J. et al. A general TR-FRET assay platform for high-throughput screening and characterizing inhibitors of methyllysine reader proteins. *SLAS Discov.* **24**, 693–700 (2019).
121. Maurel, D. et al. Cell-surface protein-protein interaction analysis with time-resolved FRET and snap-tag technologies: application to GPCR oligomerization. *Nat. Methods* **5**, 561–567 (2008).
122. Dao, T. P. T. et al. Mixing block copolymers with phospholipids at the nanoscale: from hybrid polymer/lipid wormlike micelles to vesicles presenting lipid nanodomains. *Langmuir* **33**, 1705–1715 (2017).
123. Johnson, J. L. et al. Munc13-4 Is a Rab11-binding protein that regulates Rab11-positive vesicle trafficking and docking at the plasma membrane. *J. Biol. Chem.* **291**, 3423–3438 (2016).
124. Gayrard, C. & Borghi, N. FRET-based molecular tension microscopy. *Methods* **94**, 33–42 (2016).
125. Chen, C. et al. Visualization and intracellular dynamic tracking of exosomes and exosomal miRNAs using single molecule localization microscopy. *Nanoscale* **10**, 5154–5162 (2018).
126. Oleksiuk, O. et al. Single-molecule localization microscopy allows for the analysis of cancer metastasis-specific mirna distribution on the nanoscale. *Oncotarget* **6**, 44745–44757 (2015).
127. Dabrowska, S. et al. Imaging of extracellular vesicles derived from human bone marrow mesenchymal stem cells using fluorescent and magnetic labels. *Int. J. Nanomed.* **13**, 1653–1664 (2018).
128. Willig, K. I., Rizzoli, S. O., Westphal, V., Jahn, R. & Hell, S. W. STED microscopy reveals that synaptotagmin remains clustered after synaptic vesicle exocytosis. *Nature* **440**, 935–939 (2006).
129. Chen, C. et al. Imaging and intracellular tracking of cancer-derived exosomes using single-molecule localization-based super-resolution microscope. *ACS Appl. Mater. Interfaces* **8**, 25825–25833 (2016).
130. Polanco, J. C., Li, C., Durisic, N., Sullivan, R. & Götz, J. Exosomes taken up by neurons hijack the endosomal pathway to spread to interconnected neurons. *Acta Neuropathol. Commun.* **6**, 10 (2018).
131. Gustafsson, M. G. L. Surpassing the lateral resolution limit by a factor of two using structured illumination microscopy. *J. Microsc.* **198**, 82–87 (2000).
132. Hell, S. W. Toward fluorescence nanoscopy. *Nat. Biotechnol.* **21**, 1347–1355 (2003).
133. Huang, B. Super-resolution optical microscopy: multiple choices. *Curr. Opin. Chem. Biol.* **14**, 10–14 (2010).
134. Hess, S. T., Girirajan, T. P. K. & Mason, M. D. Ultra-high resolution imaging by fluorescence photoactivation localization microscopy. *Biophys. J.* **91**, 4258–4272 (2006).
135. Nienhaus, K. & Nienhaus, G. U. Where do we stand with super-resolution optical microscopy? *J. Mol. Biol.* **428**, 308–322 (2016).
136. Bachmann, M., Fiederling, F. & Bastmeyer, M. Practical limitations of superresolution imaging due to conventional sample preparation revealed by a direct comparison of CLSM, SIM and dSTORM. *J. Microsc.* **262**, 306–315 (2016).
137. Witters, D., Knez, K., Ceyssens, F., Puers, R. & Lammertyn, J. Digital microfluidics-enabled single-molecule detection by printing and sealing single magnetic beads in femtoliter droplets. *Lab Chip* **13**, 2047–2054 (2013).
138. Gao, W., Li, X., Zeng, L. & Peng, T. Rapid isothermal detection assay: a probe amplification method for the detection of nucleic acids. *Diagn. Microbiol. Infect. Dis.* **60**, 133–141 (2008).
139. Jia, S. et al. Emerging technologies in extracellular vesicle-based molecular diagnostics. *Expert Rev. Mol. Diagn.* **14**, 307–321 (2014).
140. Chen, W. W. et al. BEAMing and droplet digital PCR analysis of mutant IDH1 mRNA in glioma patient serum and cerebrospinal fluid extracellular vesicles. *Mol. Ther. Nucleic Acids* **2**, e109 (2013).
141. Worst, T. S. et al. miR-10a-5p and miR-29b-3p as extracellular vesicle-associated prostate cancer detection markers. *Cancers (Basel)* **12**, 43 (2020).
142. Takahashi, K. et al. Circulating extracellular vesicle-encapsulated HULC is a potential biomarker for human pancreatic cancer. *Cancer Sci.* **111**, 98–111 (2020).
143. Liu, C. et al. Single-exosome-counting immunoassays for cancer diagnostics. *Nano Lett.* **18**, 4226–4232 (2018).
144. Diefenbach, R. J., Lee, J. H. & Rizos, H. Monitoring melanoma using circulating free DNA. *Am. J. Clin. Dermatol.* **20**, 1–12 (2019).
145. Kong, L., Lee, C., Earhart, C. M., Cordovez, B. & Chan, J. W. A nanotweezer system for evanescent wave excited surface enhanced Raman spectroscopy (SERS) of single nanoparticles. *Opt. Express* **23**, 6793 (2015).
146. Zong, S. et al. Facile detection of tumor-derived exosomes using magnetic nanobeads and SERS nanoprobes. *Anal. Methods* **8**, 5001–5008 (2016).
147. Lee, C., Carney, R., Lam, K. & Chan, J. W. SERS analysis of selectively captured exosomes using an integrin-specific peptide ligand. *J. Raman Spectrosc.* **48**, 1771–1776 (2017).
148. Tian, Y. F., Ning, C. F., He, F., Yin, B. C. & Ye, B. C. Highly sensitive detection of exosomes by SERS using gold nanostar@Raman reporter@nanoshell structures modified with a bivalent cholesterol-labeled DNA anchor. *Analyst* **143**, 4915–4922 (2018).
149. Zhang, W. et al. Enabling sensitive phenotypic profiling of cancer-derived small extracellular vesicles using surface-enhanced raman spectroscopy nanotags. *ACS Sens.* **5**, 764–771 (2020).

150. Schie, I. W. et al. High-throughput screening raman spectroscopy platform for label-free cellomics. *Anal. Chem.* **90**, 2023–2030 (2018).
151. Xiong, Q. et al. Magnetic nanochain integrated microfluidic biochips. *Nat. Commun.* **9**, 1743 (2018).
152. Beekman, P. et al. Immuno-capture of extracellular vesicles for individual multi-modal characterization using AFM, SEM and Raman spectroscopy. *Lab Chip* **19**, 2526–2536 (2019).
153. Rüger, J., Mondol, A. S., Schie, I. W., Popp, J. & Krafft, C. High-throughput screening Raman microspectroscopy for assessment of drug-induced changes in diatom cells. *Analyst* **144**, 4488–4492 (2019).
154. Noble, J. M. et al. Direct comparison of optical and electron microscopy methods for structural characterization of extracellular vesicles. *J. Struct. Biol.* https://doi.org/10.1016/j.jsb.2020.107474 (2020).
155. Lian, H., He, S., Chen, C. & Yan, X. Flow cytometric analysis of nanoscale biological particles and organelles. *Annu. Rev. Anal. Chem.* **12**, 389–409 (2019).
156. Chukhchin, D. G., Bolotova, K., Sinelnikov, I., Churilov, D. & Novozhilov, E. Exosomes in the phloem and xylem of woody plants. *Planta* **251**, 12 (2020).
157. Plaut, J. S. et al. Quantitative atomic force microscopy provides new insight into matrix vesicle mineralization. *Arch. Biochem. Biophys.* **667**, 14–21 (2019).
158. Arraud, N. et al. Extracellular vesicles from blood plasma: determination of their morphology, size, phenotype and concentration. *J. Thromb. Haemost.* **12**, 614–627 (2014).
159. Bevers, E. M., Comfurius, P. & Zwaal, R. F. A. Changes in membrane phospholipid distribution during platelet activation. *Biochim. Biophys. Acta* **736**, 57–66 (1983).
160. Fadok, V. A. et al. Exposure of phosphatidylserine on the surface of apoptotic lymphocytes triggers specific recognition and removal by macrophages. *J. Immunol.* **148**, 2207–2216 (1992).
161. Zwaal, R. F. A. & Schroit, A. J. Pathophysiologic implications of membrane phospholipid asymmetry in blood cells. *J. Am. Soc. Hematol.* **89**, 333–340 (1997).
162. Biró, É. et al. Human cell-derived microparticles promote thrombus formation in vivo in a tissue factor-dependent manner. *J. Thromb. Haemost.* **1**, 2561–2568 (2003).
163. Morel, O., Jesel, L., Freyssinet, J. M. & Toti, F. Cellular mechanisms underlying the formation of circulating microparticles. *Arterioscler. Thromb. Vasc. Biol.* **31**, 15–26 (2011).
164. Emelyanov, A. et al. Cryo-electron microscopy of extracellular vesicles from cerebrospinal fluid. *PLoS ONE* **15**, e0227949 (2020).
165. Yekula, A. et al. Large and small extracellular vesicles released by glioma cells *in vitro* and *in vivo*. *J. Extracell. Vesicles* **9**, 1689784 (2020).
166. Thane, K. E., Davis, A. M. & Hoffman, A. M. Improved methods for fluorescent labeling and detection of single extracellular vesicles using nanoparticle tracking analysis. *Sci. Rep.* **9**, 12295 (2019).
167. Dragovic, R. A. et al. Isolation of syncytiotrophoblast microvesicles and exosomes and their characterisation by multicolour flow cytometry and fluorescence nanoparticle tracking analysis. *Methods* **87**, 64–74 (2015).
168. Koifman, N., Biran, I., Aharon, A., Brenner, B. & Talmon, Y. A direct-imaging cryo-EM study of shedding extracellular vesicles from leukemic monocytes. *J. Struct. Biol.* **198**, 177–185 (2017).
169. LeClaire, M., Gimzewski, J. & Sharma, S. A review of the biomechanical properties of single extracellular vesicles. *Nano Sel.* https://doi.org/10.1002/nano.202000129 (2020).
170. Royo, F. et al. Differences in the metabolite composition and mechanical properties of extracellular vesicles secreted by hepatic cellular models. *J. Extracell. Vesicles* **8**, 1575678 (2019).
171. Logozzi, M. et al. Microenvironmental pH and exosome levels interplay in human cancer cell lines of different histotypes. *Cancers (Basel)* **10**, 370 (2018).
172. Royo, F. et al. Transcriptomic profiling of urine extracellular vesicles reveals alterations of CDH3 in prostate cancer. *Oncotarget* **7**, 6835–6846 (2016).
173. Federici, C. et al. Exosome release and low pH belong to a framework of resistance of human melanoma cells to cisplatin. *PLoS ONE* **9**, e88193 (2014).
174. Oosthuyzen, W. et al. Quantification of human urinary exosomes by nanoparticle tracking analysis. *J. Physiol.* **591**, 5833–5842 (2013).
175. Logozzi, M. et al. Increased PSA expression on prostate cancer exosomes in in vitro condition and in cancer patients. *Cancer Lett.* **403**, 318–329 (2017).
176. Logozzi, M., Spugnini, E., Mizzoni, D., Di Raimo, R. & Fais, S. Extracellular acidity and increased exosome release as key phenotypes of malignant tumors. *Cancer Metastasis Rev.* **38**, 93–101 (2019).
177. Calorini, L., Peppicelli, S. & Bianchini, F. Extracellular acidity as favouring factor of tumor progression and metastatic dissemination. *Exp. Oncol.* **34**, 79–84 (2012).
178. Huber, V. et al. Cancer acidity: an ultimate frontier of tumor immune escape and a novel target of immunomodulation. *Semin. Cancer Biol.* **43**, 74–89 (2017).
179. Padda, R. S. et al. Nanoscale flow cytometry to distinguish subpopulations of prostate extracellular vesicles in patient plasma. *Prostate* **79**, 592–603 (2019).
180. Xian, Y., Zhou, M., Han, S., Yang, R. & Wang, Y. A FRET biosensor reveals free zinc deficiency in diabetic beta-cell vesicles. *Chin. Chem. Lett.* **31**, 468–472 (2020).
181. Nguyen, D. B. et al. Characterization of microvesicles released from human red blood cells. *Cell. Physiol. Biochem.* **38**, 1085–1099 (2016).
182. Polanco, J. C., Scicluna, B. J., Hill, A. F. & Götz, J. Extracellular vesicles isolated from the brains of rTg4510 mice seed tau protein aggregation in a threshold-dependent manner. *J. Biol. Chem.* **291**, 12445–12466 (2016).
183. Wang, Y. et al. The release and trans-synaptic transmission of Tau via exosomes. *Mol. Neurodegener.* **12**, 5 (2017).
184. Yang, J. E. et al. Complexity and ultrastructure of infectious extracellular vesicles from cells infected by non-enveloped virus. *Sci. Rep.* **10**, 7939 (2020).
185. Santos, M. F. et al. VAMP-associated protein-A and oxysterol-binding protein–related protein 3 promote the entry of late endosomes into the nucleoplasmic reticulum. *J. Biol. Chem.* **293**, 13834–13848 (2018).
186. Mannavola, F. et al. Tumor-derived exosomes promote the in vitro osteotropism of melanoma cells by activating the SDF-1/CXCR4/CXCR7 axis. *J. Transl. Med.* **17**, 230 (2019).
187. Sorkin, R. et al. Nanomechanics of extracellular vesicles reveals vesiculation pathways. *Small* **14**, e1801650 (2018).
188. Vorselen, D. et al. The fluid membrane determines mechanics of erythrocyte extracellular vesicles and is softened in hereditary spherocytosis. *Nat. Commun.* **9**, 4960 (2018).
189. Böcking, T., Upadhyayula, S., Rapoport, I., Capraro, B. R. & Kirchhausen, T. Reconstitution of clathrin coat disassembly for fluorescence microscopy and single-molecule analysis. *Methods Mol. Biol.* **1847**, 121–146 (2018).
190. Mattheyses, A. L., Atkinson, C. E. & Simon, S. M. Imaging single endocytic events reveals diversity in clathrin, dynamin, and vesicle dynamics. *Traffic* **12**, 1394–1406 (2011).
191. Van Lengerich, B., Rawle, R. J., Bendix, P. M. & Boxer, S. G. Individual vesicle fusion events mediated by lipid-anchored DNA. *Biophys. J.* **105**, 409–419 (2013).
192. Mattie, S., Kazmirchuk, T., Mui, J., Vali, H. & Brett, C. L. Visualization of SNARE-mediated organelle membrane hemifusion by electron microscopy. *Methods Mol. Biol.* **1860**, 361–377 (2019).

193. Hu, Y., Tian, Z. & Diao, J. Single-molecule fluorescence measurement of SNARE-mediated vesicle fusion. in *SNAREs: Methods and Protocols* (ed. Fratti, R.) 335–344 (2019).
194. Lin, C. C. et al. Control of membrane gaps by synaptotagmin-Ca 2+ measured with a novel membrane distance ruler. *Nat. Commun.* **5**, 5859 (2014).
195. Stratton, B. S. et al. Cholesterol increases the openness of SNARE-mediated flickering fusion pores. *Biophys. J.* **110**, 1538–1550 (2016).
196. Cao, H. et al. In vivo real-time imaging of extracellular vesicles in liver regeneration via aggregation-induced emission luminogens. *ACS Nano* **13**, 3522–3533 (2019).
197. Lai, C. P. et al. Dynamic biodistribution of extracellular vesicles in vivo using a multimodal imaging reporter. *ACS Nano* **8**, 483–494 (2014).
198. Gangadaran, P., Hong, C. M. & Ahn, B. C. Current perspectives on in vivo noninvasive tracking of extracellular vesicles with molecular imaging. *Biomed Res. Int.* **2017**, (2017).
199. Lai, C. P., Tannous, B. A. & Breakefield, X. O. Noninvasive in vivo monitoring of extracellular vesicles. in. *Methods Mol. Biol.* **1098**, 249–258 (2014).
200. Van Der Vos, K. E. et al. Directly visualized glioblastoma-derived extracellular vesicles transfer RNA to microglia/macrophages in the brain. *Neuro. Oncol.* **18**, 58–69 (2016).
201. Ricklefs, F. L. et al. Imaging flow cytometry facilitates multiparametric characterization of extracellular vesicles in malignant brain tumours. *J. Extracell. Vesicles* **8**, 1588555 (2019).
202. Lai, C. P. et al. Visualization and tracking of tumour extracellular vesicle delivery and RNA translation using multiplexed reporters. *Nat. Commun.* **6**, 7029 (2015).
203. Verweij, F. J., Hyenne, V., Van Niel, G. & Goetz, J. G. Extracellular vesicles: catching the light in zebrafish. *Trends Cell Biol.* **29**, 770–776 (2019).
204. Kobayashi-Sun, J. et al. Uptake of osteoblast-derived extracellular vesicles promotes the differentiation of osteoclasts in the zebrafish scale. *Commun. Biol.* **3**, 190 (2020).
205. Sung, B. H. et al. A live cell reporter of exosome secretion and uptake reveals pathfinding behavior of migrating cells. *Nat. Commun.* **11**, 2092 (2020).
206. Clos-Garcia, M. et al. Gut microbiome and serum metabolome analyses identify molecular biomarkers and altered glutamate metabolism in fibromyalgia. *EBioMedicine* **46**, 499–511 (2019).
207. Roman-Canal, B. et al. EV-associated miRNAs from peritoneal lavage are a source of biomarkers in endometrial cancer. *Cancers (Basel).* **11**, 839 (2019).
208. Tian, Y. et al. Protein profiling and sizing of extracellular vesicles from colorectal cancer patients via flow cytometry. *ACS Nano* **12**, 671–680 (2018).
209. Clos-Garcia, M. et al. Integrative analysis of fecal metagenomics and metabolomics in colorectal cancer. *Cancers (Basel)* **12**, 1142 (2020).
210. Royo, F. & Falcon-Perez, J. M. Liver extracellular vesicles in health and disease. *J. Extracell. Vesicles* https://doi.org/10.3402/jev.v1i0.18825 (2012).
211. He, D. et al. Total internal reflection-based single-vesicle in situ quantitative and stoichiometric analysis of tumor-derived exosomal microRNAs for diagnosis and treatment monitoring. *Theranostics* **9**, 4494–4507 (2019).
212. Murakami, Y. et al. Comprehensive miRNA expression analysis in peripheral blood can diagnose liver disease. *PLoS ONE* **7**, e48366 (2012).
213. Pang, B. et al. Extracellular vesicles: the next generation of biomarkers for liquid biopsy-based prostate cancer diagnosis. *Theranostics* **10**, 2309–2326 (2020).
214. Vlaeminck-Guillem, V. Extracellular vesicles in prostate cancer carcinogenesis, diagnosis, and management. *Front. Oncol.* **8**, 222 (2018).
215. Mateo, L., Guitart-Pla, O., Duran-Frigola, M. & Aloy, P. Exploring the OncoGenomic Landscape of cancer. *Genome Med.* **10**, 61 (2018).
216. Joncas, F. H. et al. Plasma extracellular vesicles as phenotypic biomarkers in prostate cancer patients. *Prostate* **79**, 1767–1776 (2019).
217. Carlsson, J. et al. Validation of suitable endogenous control genes for expression studies of miRNA in prostate cancer tissues. *Cancer Genet. Cytogenet.* **202**, 71–75 (2010).
218. Schaefer, A. et al. Suitable reference genes for relative quantification of miRNA expression in prostate cancer. *Exp. Mol. Med.* **42**, 749–758 (2010).
219. Haka, A. S. et al. Diagnosing breast cancer by using Raman spectroscopy. *Proc. Natl Acad. Sci. USA* **102**, 12371–12376 (2005).
220. Haka, A. S. et al. Diagnosing breast cancer using Raman spectroscopy: prospective analysis. *J. Biomed. Opt.* **14**, 054023 (2009).
221. Notarangelo, M. et al. Ultrasensitive detection of cancer biomarkers by nickel-based isolation of polydisperse extracellular vesicles from blood. *EBioMedicine* **43**, 114–126 (2019).
222. Melo, S. A. et al. Glypican1 identifies cancer exosomes and facilitates early detection of cancer. *Nature* **523**, 177–182 (2015).
223. Biggs, C. N. et al. Prostate extracellular vesicles in patient plasma as a liquid biopsy platform for prostate cancer using nanoscale flow cytometry. *Oncotarget* **7**, 8839–8849 (2016).
224. Cannon, D. M., Winograd, J. N. & Ewing, A. G. Quantitative chemical analysis of single cells. *Annu. Rev. Biophys. Biomol. Struct.* **29**, 239–263 (2000).
225. Li, X., Dunevall, J. & Ewing, A. G. Quantitative chemical measurements of vesicular transmitters with electrochemical cytometry. *Acc. Chem. Res.* **49**, 2347–2354 (2016).
226. Li, X., Dunevall, J., Ren, L. & Ewing, A. G. Mechanistic aspects of vesicle opening during analysis with vesicle impact electrochemical cytometry. *Anal. Chem.* **89**, 9416–9423 (2017).
227. Ranjbari, E. et al. Direct measurement of total vesicular catecholamine content with electrochemical microwell arrays. *Anal. Chem.* **92**, 11325–11331 (2020).
228. Dunevall, J., Majdi, S., Larsson, A. & Ewing, A. Vesicle impact electrochemical cytometry compared to amperometric exocytosis measurements. *Curr. Opin. Electrochem* **5**, 85–91 (2017).
229. Li, X., Majdi, S., Dunevall, J., Fathali, H. & Ewing, A. G. Quantitative measurements of transmitters in vesicles one at a time in single cell cytoplasm with nano-tip electrodes. *Angew. Chem. Int. Ed. Engl.* **54**, 11978–11982 (2015).
230. Li, X., Dunevall, J. & Ewing, A. G. Electrochemical quantification of transmitter concentration in single nanoscale vesicles isolated from PC12 cells. *Faraday Discuss* **210**, 353–364 (2018).
231. Ren, L. et al. Zinc regulates chemical-transmitter storage in nanometer vesicles and exocytosis dynamics as measured by amperometry. *Angew. Chem. Int. Ed. Engl.* **56**, 4970–4975 (2017).
232. Li, X., Dunevall, J. & Ewing, A. G. Using single-cell amperometry to reveal how cisplatin treatment modulates the release of catecholamine transmitters during exocytosis. *Angew. Chem.* **128**, 9187–9190 (2016).
233. Zupanc, J., Bas, E. & Erdogmus, D. Analysis of lipid vesicle populations from microscopy video sequences. *2010 Annu. Int. Conf. IEEE Eng. Med. Biol. Soc. EMBC'10* 5050–5053 https://doi.org/10.1109/IEMBS.2010.5626223 (2010)
234. Barriere, H. & Lukacs, G. L. Analysis of endocytic trafficking by single-cell fluorescence ratio imaging. *Curr. Protoc. Cell Biol.* https://doi.org/10.1002/0471143030.cb1513s40 (2008)
235. Chen, T. *et al.* Microwave biosensor dedicated to the dielectric spectroscopy of a single alive biological cell in its culture medium. in *Microwave Symposium Digest (IMS), 2013 IEEE MTT-S International* (2013).

236. Chen, W., Dubuc, D. & Grenier, K. Parametric study of a microwave sensor dedicated to the dielectric spectroscopy of single particles and biological cells. in *2015 European Microwave Conference (EuMC 2015)* 829–832 (2015).
237. Chen, W., Dubuc, D. & Grenier, K. Impact of sensor metal thickness on microwave spectroscopy sensitivity for individual particles and biological cells analysis. in *2016 IEEE Topical Conference on Biomedical Wireless Technologies, Networks, and Sensing Systems (BioWireleSS)* 81–83 (2016).
238. Zhang, M. *et al.* Electrically controlled tunable broadband interferometric dielectric spectroscopy: groundwork for single cell analysis. in *2019 49th European Microwave Conference (EuMC)* 650–653 (2019).
239. Cui, Y. et al. Analyzing single giant unilamellar vesicles with a slotline-based RF nanometer sensor. *IEEE Trans. Microw. Theory Tech.* **64**, 1339–1347 (2016).
240. Wu, M. et al. Isolation of exosomes from whole blood by integrating acoustics and microfluidics. *Proc. Natl Acad. Sci. USA* **114**, 10584–10589 (2017).
241. Ku, A. et al. Acoustic enrichment of extracellular vesicles from biological fluids. *Anal. Chem.* **90**, 8011–8019 (2018).
242. Ku, A. et al. A urinary extracellular vesicle microRNA biomarker discovery pipeline; from automated extracellular vesicle enrichment by acoustic trapping to microRNA sequencing. *PLoS ONE* **14**, e0217507 (2019).
243. Carter, E. P. et al. Visualizing Ebolavirus particles using single-particle interferometric reflectance imaging sensor (SP-IRIS). in *Ebolaviruses: Methods and Protocols* (eds. Groseth, A. & Hoenen, T.) 373–393 (Springer, 2017).
244. Ünlü, N. L., Kanik, F. E., Seymour, E., Connor, J. H. & Ünlü, M. S. DNA-directed antibody immobilization for robust protein microarrays: application to single particle detection DNA-directed antibody immobilization. in *Biosensors and Biodetection: Methods and Protocols* (eds. Rasooly, A. & Prickril, B.) 187–206 (Springer, 2017).
245. Akagi, T. et al. On-chip immunoelectrophoresis of extracellular vesicles released from human breast cancer cells. *PLoS ONE* **10**, e0123603 (2015).
246. Friedrich, R. et al. A nano flow cytometer for single lipid vesicle analysis. *Lab Chip* **17**, 830–841 (2017).
247. Obeid, S. et al. NanoBioAnalytical characterization of extracellular vesicles in 75-nm nanofiltered human plasma for transfusion: a tool to improve transfusion safety. *Nanomedicine* **20**, 10197 (2019).
248. Yokota, S. et al. Extracellular vesicles nanoarray technology: immobilization of individual extracellular vesicles on nano-patterned polyethylene glycol-lipid conjugate brushes. *PLoS ONE* **14**, e0224091 (2019).
249. Ji, Y. et al. Multiplexed profiling of single-cell extracellular vesicles secretion. *Proc. Natl Acad. Sci. USA* **116**, 5979–5984 (2019).
250. Bai, Y. et al. Absolute quantification and analysis of extracellular vesicle lncRNAs from the peripheral blood of patients with lung cancer based on multi-colour fluorescence chip-based digital PCR. *Biosens. Bioelectron.* **142**, 111523 (2019).
251. Akagi, T., Kato, K., Hanamura, N., Kobayashi, M. & Ichiki, T. Evaluation of desialylation effect on zeta potential of extracellular vesicles secreted from human prostate cancer cells by on-chip microcapillary electrophoresis. *Jpn. J. Appl. Phys.* **53**, 06JL01 (2014).
252. Weber, A., Wehmeyer, J. C., Schmidt, V., Lichtenberg, A. & Akhyari, P. Rapid fluorescence-based characterization of single extracellular vesicles in human blood with nanoparticle-tracking analysis. *J. Vis. Exp.* https://doi.org/10.3791/58731 (2019).
253. Marku, A. et al. The LRRK2 N-terminal domain influences vesicle trafficking: impact of the E193K variant. *Sci. Rep.* **10**, 3799 (2020).

Acknowledgements

The authors of this review were supported by funds from the European Union's Horizon 2020 research and innovation programme under grant agreement no. 860303. We thank MINECO for the TenTaCles (Spanish Excellence Network in Exosomes) and the Severo Ochoa Excellence Accreditation (SEV-2016-0644). This project has received funding from the Spanish Ministry of Economy and Competitiveness MINECO (RTI2018-094969-B-I00).

Author contributions

All of the authors wrote, edited and discussed this review.

Competing interests

The authors declare no competing interests.

Additional information

Correspondence and requests for materials should be addressed to G.B.-F. or J.M.F.-P.

Peer review information *Nature Protocols* thanks Paolo Bergese, Cees Otto and Frederik Johannes Verweij for their contribution to the peer review of this work.

Reprints and permissions information is available at www.nature.com/reprints.

Publisher's note Springer Nature remains neutral with regard to jurisdictional claims in published maps and institutional affiliations.

Received: 27 July 2020; Accepted: 31 March 2021;
Published online: 16 June 2021

Related links

Key references using this protocol

Kruglik, S. G. et al. *Nanoscale* **11**, 1661–1679 (2019): https://doi.org/10.1039/C8NR04677H
Royo, F. et al. *J. Extracell. Vesicles* **8**, 1575678 (2019): https://doi.org/10.1080/20013078.2019.1575678
Tatischeff, I., Larquet, E., Falcon-Perez, J. M., Turpin, P.-Y. & Kruglik, S. G. *J. Extracell. Vesicles* **1**, 19179 (2012): https://doi.org/10.3402/jev.v1i0.19179